rapidFLIM HiRes

Redefining standards for dynamic FLIM imaging

SEE THE CHANGE.

SEE IT PRECISELY.

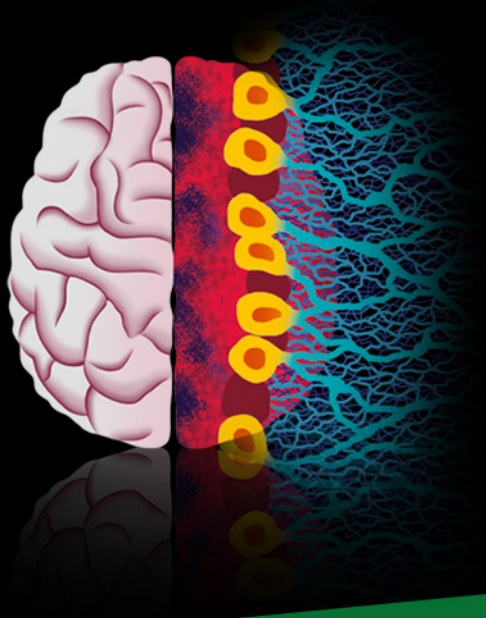

SEE IT CONFOCAL.

DOWNLOAD Free White Paper

PicoQuant

Journal of Microscopy

Journal of Microscopy, Vol. 281, Issue 2 2021, pp. 138–156 doi: 10.1111/jmi.12951
Received 7 May 2020; accepted 28 July 2020

An introduction to cryo-FIB-SEM cross-sectioning of frozen, hydrated Life Science samples

M.F. HAYLES* & D.A.M. DE WINTER†
*Cryo-FIB-SEM Technologist, Eindhoven, the Netherlands
†Environmental Hydrogeology, Department of Earth Sciences, Faculty of Geosciences, Utrecht University, Utrecht, the Netherlands

Key words. Cross-section, cryo-FIB-SEM, cryo-fracture, FIB-SEM, serial-sectioning, site-specific X-sectioning, vitrification.

Summary

The introduction of cryo-techniques to the focused ion-beam scanning electron microscope (FIB-SEM) has brought new opportunities to study frozen, hydrated samples from the field of Life Sciences. Cryo-techniques have long been employed in electron microscopy. Thin electron transparent sections are produced by cryo-ultramicrotomy for observation in a cryo-transmission electron microscope (TEM). Cryo-TEM is presently reaching the imaging of macromolecular structures. In parallel, cryo-fractured surfaces from bulk materials have been investigated by cryo-SEM.

Both cryo-TEM and cryo-SEM have provided a wealth of information, despite being 2D techniques. Cryo-TEM tomography does provide 3D information, but the thickness of the volume has a maximum of 200–300 nm, which limits the 3D information within the context of specific structures. FIB-milling enables imaging additional planes by creating cross-sections (e.g. cross-sectioning or site-specific X-sectioning) perpendicular to the cryo-fracture surface, thus adding a third imaging dimension to the cryo-SEM. This paper discusses how to produce suitable cryo-FIB-SEM cross-section results from frozen, hydrated Life Science samples with emphasis on 'common knowledge' and reoccurring observations.

Introduction

Visualising structures of cells and tissue by the scanning electron microscope (SEM) has been a great help in understanding many processes studied by Life Sciences (Schatten, 2012). A common challenge in cell biology, botany and medical applications is the hydrated nature of the sample, which is incompatible with the vacuum conditions required for high-end SEM imaging. Two general solutions are available: (1) extracting the water, optionally being replaced by a resin and (2) cryo-fixate the hydrated sample and maintain the frozen condition in the SEM (Schatten, 2012). Note that cryo-fixation is also used in processes of extracting and/or replacing the water phase (e.g. freeze drying, freeze substitution) to ultimately obtain a sample that can be investigated by room temperature electron microscopy. In the present paper, we focus on samples that remain hydrated and are kept frozen during the investigation by cryo-focused ion beam-SEM (cryo-FIB-SEM). For many decades, frozen samples were fractured at low temperatures in a vacuum environment in order to create a fresh surface to be imaged by cryo-SEM (Walther, 2003). Cryo-fracturing requires some good fortune in fracturing across a particular feature, while interpretation can be hampered by surface roughness and debris from the fracture. The introduction of the FIB in this process enables one to produce cross-sections perpendicular to the fracture surface. FIB cross-sections are free from debris and roughness related to fracturing. Consequently, FIB-milling and subsequent SEM imaging reveals highly detailed structural information of the sample while maintaining cryogenic temperatures.

This paper encompasses the practical insight of how to FIB-mill and SEM-image a cross-section of a frozen hydrated Life Science sample with cryo-FIB-SEM. A sample of yeast (*Saccharomyces Cerevisiae*) has been frequently used for practical purposes and to demonstrate the processes, techniques and problems encountered. Executing a cryo-FIB-SEM experiment involves a variety of instruments, techniques and some experience. Certain choices to make are tightly linked to the specific type of sample and the related scientific research. The number of steps from start to finish is frequently perceived as intimidating to noncryo-FIB-SEM specialists. However, all the individual steps are actually rather straightforward and easily deducible through simple reasoning. The techniques in this paper are the basis of all cryo-FIB-SEM methods. While the cryo-FIB-SEM community has ventured into new applications, as discussed elsewhere in this special issue (Kuba *et al.*,

Correspondence to: D. A. M. De Winter, Environmental Hydrogeology, Department of Earth Sciences, Faculty of Geosciences, Utrecht University, Vening Meineszgebouw A, Princetonlaan 8a, 3584 CB Utrecht, The Netherlands. Tel: +3130 253 7973; e-mail: D.A.M.deWinter@uu.nl

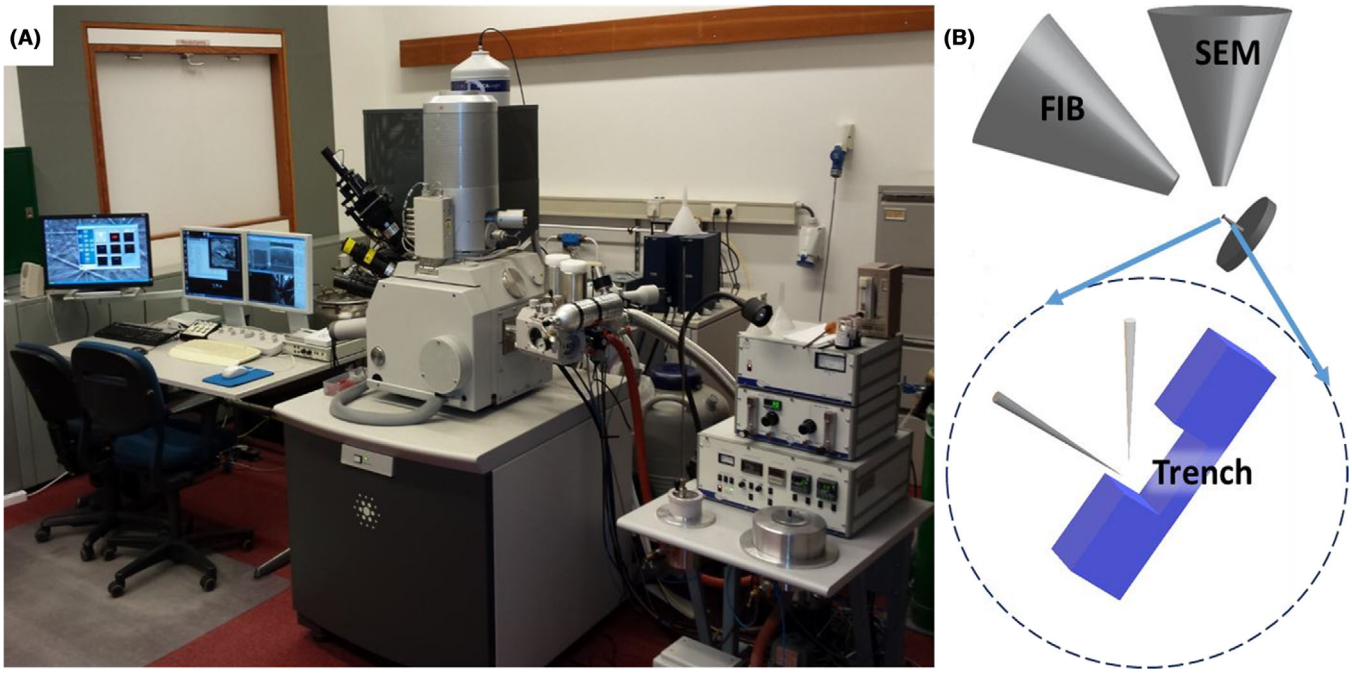

Fig. 1. Cryo-FIB-SEM setup: (A) The FIB-SEM as installed at Utrecht University. In the middle the microscope itself and to the right additional hardware related to the cryo-transfer system. Most of the results shown in this paper are obtained with this setup. (B) Schematic representation of the position of the sample with respect to the FIB and SEM. Both beams view the same location on the sample when the eucentric position is used. Working at the eucentric position is beneficial, as the SEM can check the progress of ongoing FIB-milling actions.

2020; Parmenter, 2020; De Winter *et al.*, 2020), we felt that a 'proper introduction' into the subject is required, both as a reference to experienced users as well as inspiration to, and support for, newcomers in the field.

Instrumentation

FIB-SEM's are made by a number of manufacturers: Thermo Fisher Scientific (formerly FEI), Portland, Oregon, USA, Hitachi, Jeol, Tescan and Zeiss. Cryo-equipment used with most of the FIB-SEMs is usually from another manufacturer and has to be tailored to the design and specific properties of the FIB-SEM chamber layout, as well as satisfy the research objective. Present cryo-transfer system manufacturers have reduced in number over the last few years, with Quorum (Quorum Technologies Ltd., Laughton, East Sussex, UK) and Leica (Leica Microsystems, Vienna, Austria) remaining. The authors realise that there are still various combinations of FIB-SEMs with cryo-transfer systems from past and present manufacturers in the field. We like to stress that all principles are generic and should be transferable to former or more recent models of instrumentation, although some details may be geared towards specific instrumental characteristics. The work presented in this paper is largely obtained from a FEI Nova Nanolab 600 Dual beam in combination with a Quorum PP2000T cryo-transfer system (Fig. **1A**).

Cryo-FIB-SEM

The FIB-SEM instrument is a full integration of two columns, a liquid-metal-ion source (gallium ions) column for FIB-milling and a highly spatially resolving SEM with a Field Emission Gun (FEG) electron column for imaging. All cryo-FIB-SEM operations occur at low pressures (10^{-5} mbar–10^{-7} mbar) to ensure free pathways for both the ion and electron beams.

The FIB consists of a beam of accelerated gallium ions which is focused on the surface of the sample. The momentum transfer of the gallium ions to the sample causes sputtering of the sample's native atoms, thus providing a mechanism to produce cross-sections (Volkert & Minor, 2007). The ratio between the incoming ions and the sputtered atoms is called the sputter yield and is a measure for the speed of the milling process (Mulders *et al.*, 2007). Ice mills particularly fast (Marko *et al.*, 2005; Fu *et al.*, 2008). Hence, the dimensions of cross-sections in frozen, hydrated samples can easily be some hundred microns wide and a few tens of microns deep. The SEM provides an accelerated, focused electron beam that scans across the surface of the sample (Reimer, 1998). The primary electrons from the beam are elastically scattered at impact by the nuclei of the sample's atoms. As a result, some primary electrons escape from below the surface, becoming backscattered electrons (BSE). BSE carry information about the atomic weight, density and crystallographic orientation of the target volume. From the same target location come

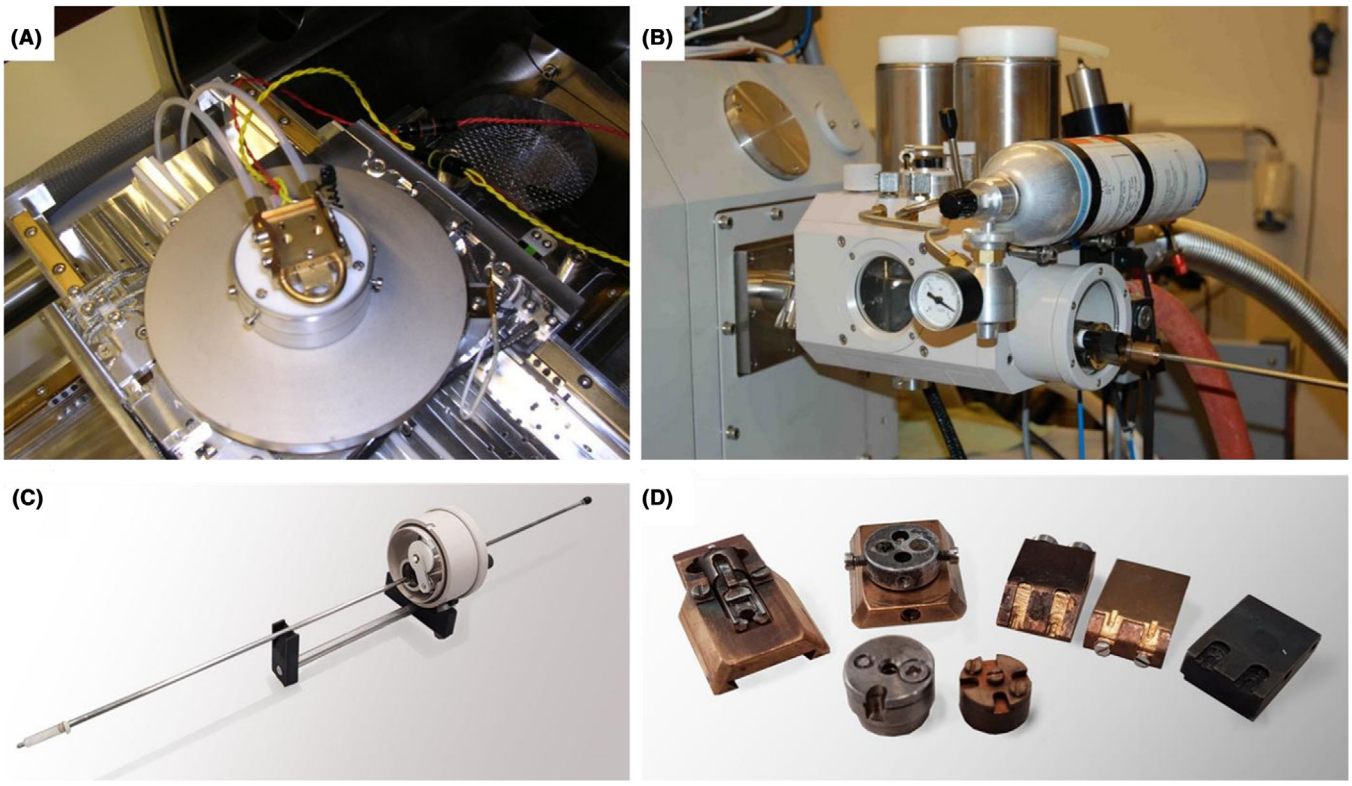

Fig. 2. Cryo-transfer hardware: (A) The cryo-stage with inlet/outlet tubes for the cold Nitrogen gas and electrical connections for the temperature read-out and heating element. (B) The Quorum PP2000T prep chamber with freeze fracturing, sublimation, sputter coating facilities and enabling a cold, vacuum transfer into the FIB-SEM chamber. (C) The transfer rod is used to interface between the freezing unit (external), the prep chamber and the Microscope chamber. (D) The cryo-holder/sledge comes in a variety of types for different applications and can contain one or more samples. Customizing these parts is easy and may be necessary to suit the experiment.

inelastically scattered secondary electrons (SE). SEs are defined by their energy which per convention ranges from >0 eV to 50 eV. SE's can only escape from the sample into the vacuum when generated very close to the surface. Hence SE's are very susceptible to surface roughness. Other generated signal types are X-rays, cathodoluminescence and Auger electrons, but these are not relevant to the present discussion.

Mechanical and electronic alignments ensure a specific working distance with respect to the electron column where the ion and electron beam coincide. It is also very advantageous to work a eucentric-tilt position, which is usually at the same position (Fig. **1B**). This allows use of the SEM to monitor the milling action of the FIB. Operation of FIB-milling is discussed later (see 'FIB-milling' section).

The cryo-transfer system

Commercially available cryo-transfer systems consist of a number of components. Some of these components are common in purpose while others define the approach to the cooling method and transfer utilised by the manufacturer.

Inside the vacuum chamber. At the heart of the cryo-transfer-system is the cryo-stage and anti-contaminator. The cryo-stage is normally fitted on top of the standard FIB-SEM stage (after removing the stub holder). The anti-contaminator is usually mounted around the pole piece of the electron column, shielding the sample from the warm surface of the electron column. The anti-contaminator is sometimes called the 'cold-trap', which should be at a lower temperature than the sample in order to 'trap' contaminants from reaching the sample. Stage movements can still be made through the normal stage movement operations provided by the FIB-SEM manufacturer (Fig. **2A**). Only the rotation is limited due to the electrical connections and tubing or metal braids attached to the cryo-stage, except when using a cryo-rotation stage (Hayles *et al.*, 2010; Rigort *et al.*, 2010a). The top part of the cryo-stage is actively cooled and accommodates the sample holder. The similarities between different manufactures ends here, as the cooling methods used are different.

Gas flow. N_2 gas is cooled by an external heat exchanger which is submerged in a liquid nitrogen (LN_2) filled dewar. Tubes carrying the cooled gas from the heat exchanger run directly through the anti-contaminator and the cryo-stage,

delivering the cold temperatures needed. The cryo-stage has a heater that can regulate the low temperature to that required. Quorum Technologies developed long-duration constant-gas-flow cooling.

Conduction. A large metal block, which acts as a heat sink, is cooled down by a dewar filled with LN_2 mounted outside the microscope chamber. Metal braids (often copper) connect the block to the cryo-stage and anti-contaminator. Leica Microsystems uses conduction to cool the cryo-stage.

The advantage of cooling the cryo-stage with N_2 gas in combination with a heater is that it delivers fast and accurate control of the temperature. Braids are inherently slower in responding to (deliberate) temperature changes. Although both gas flow and conduction are susceptible to vibrations, both methods have been proven to function vibration-free.

A generic requirement for cryo-transfer systems is the ability to maintain a constant temperature throughout the day. Temperature changes will cause stage drift due to contraction/expansion of the metal components of the stage. A ball-park figure for the required stability is less than 1 °C per 3 h. Fast and accurate control over the temperatures allows for sublimation strategies (see 'Sublimation strategy' section). The sublimation cycle uses a heating element in the cryo-stage to heat up the sample to for example −90 °C without changing the flow of N_2 gas. Once the required sublimation is finished, the heating element is switched off and the temperature quickly falls back to the original temperature based on the N_2 gas flow. Braid-based systems may be less suitable for *in situ* sublimation due to the relatively slow recovery of the temperature. Sublimation can be performed *ex situ*, although monitoring the process live with the SEM is then no longer possible. It is also advantageous to be able to control the temperature of the anti-contaminator independently from the cryo-stage. In general, it is advised to maintain a temperature for the anti-contaminator that is 20 °C lower than the specimen temperature.

Outside the vacuum chamber. Attached to the FIB-SEM vacuum chamber is a transfer module, allowing for transferring a previously frozen sample into the vacuum chamber. The transfer module ensures maintaining a low temperature and protects the sample from air/moisture (Fig. **2B**). All commercially available cryo-transfer systems use some sort of sample-holder transfer mechanism (Fig. **2C**).

Hydrated samples have to be frozen before entering the vacuum chamber. Various freezing techniques are available, which are discussed in 'Sample preparation procedures' section. The sample is kept submerged in LN_2 once frozen and placed, if not already, onto the sample holder (sledge) (Fig. **2D**). Attaching the sample holder to the transfer rod is usually done in a special unit that allows for pumping down of the transfer device. Subsequently, the sample holder is transferred to the cryo-FIB-SEM under vacuum conditions. In many cases, it is required to create a fresh freeze-fracture surface and to apply a sputter coating to ensure electrical conduction of the sample surface. Again, a clear distinction can be found in solutions offered by different manufacturers. Present and past makers of gas-flow cryo-transfer systems offer a cryo-preparation chamber connected to the transfer module that is attached to the microscope chamber. The cryo-preparation chamber carries facilities for sputter coating, freeze fracturing, manual manipulation of the sample and sublimation cycles. As such, the cryo-preparation chamber is part of the transfer route for the sample into the microscope chamber. Manufacturers of conduction-based cryo-transfer system chose to offer a separate unit ('off-column') for the same processes. The shuttle device for transferring the sample into the microscope chamber can be used to interface the separate bench-mounted preparation units.

Finally, an ideal transfer moves from warm to cold. With the cryo-stage set to a certain temperature (e.g. −160 °C), ideally the incoming sample from the cryo-preparation stage should be controlled around the same temperature. If the sample is too cold, it may act as a cold-trap and accumulate ice on the sample surface from water vapour left in the vacuum chamber. If the sample is too warm, it will slowly sublime the sample surface of water (ice). Colder and warmer samples alike can offset the temperature of the cryo-stage, initially requiring the cryo-stage to settle again at a constant temperature. Resettling of a large temperature difference can cause temporary stage drift.

Tips for setting up instrumentation before a cryo-session

Many FIB-SEM microscopes are used both for room temperature and cryogenic work. Consequently, cryo-equipment is routinely mounted and dismounted. Whether or not a FIB-SEM is utilised as a dedicated cryo-microscope depends on the lab and their fields of application. In this paper, we assume that a cryo-stage is installed regularly.

Before starting a cryo-session, some, if not all of these following items may need attention, depending on the equipment being used.

Stage calibration. Most FIB-SEM systems have a computer-controlled motorised stage. It is advantageous to run a stage calibration procedure preferably prior to the installation of the cryo-stage. Recalibration brings back the stage to its original position, which facilitates a reproducible relocation of previous runs of the cryo-stage. In addition, the procedure may prevent stage tracking errors.

Crucible temperature. It is advantageous to set the temperature of the crucible to the correct temperature in case *in situ* gas-assisted deposition will be used (see 'Sample protection' section). Installing the stage and setting the crucible temperature is best done one day prior to the experiment. Some crucibles automatically warm up when the software is launched. Heating is usually fast, but cooling down can take several

hours. The standard operational temperature of the crucible for Pt deposition is 47 °C, whereas an operational temperature of 28 °C is required for Pt deposition under cryo-conditions. If the FIB-SEM is mainly used for cryo-experiments, the temperature of 28 °C can be set as default in the control software.

Stiffness of nitrogen tubing. For gas flow systems, the tubes that carry N_2 gas to and from the cryo-stage will become very stiff upon cooling. Once cold, the tubes can push or pull on the cryo-stage when the operator attempts to move the cryo-stage over some lateral distances or during tilting or rotating of the stage. Therefore, it is advantageous to swing the tubes around within the microscope chamber, distributing the force over a greater length of tube, which reduces the torque on the stage. The specific track of the tubes depends on the specific geometry of the interior of the FIB-SEM. Care must be taken that the tubes do not become trapped behind any protruding component within the vacuum chamber.

Pump down time. Once the installation of the cryo-hardware components is finished, we advise to leave the system pumping for at least 6–8 h (typically overnight) in order to pump out as much water vapour as possible. Long-term pumping will avoid a significant portion of unwanted ice contamination from water trapped on surfaces that have been previously exposed to atmosphere during the first session (see 'Contamination from the atmosphere' section). The microscope chamber should not be opened again after assembly of the cryo-stage and anti-contaminator, until the end of the cryo-session. It is advised not to open the chamber while the stage or anti-contaminator is cold, as large amounts of water vapour will rapidly condense onto the cold surfaces. The subsequent pumping down time will be very long, due to slow sublimation of the mass of condensed ice.

Water-free N_2 gas supply. Preferably, the N_2 gas supply should come from a pressurised Dewar or from an 'in-house' N_2 gas supply (typically from the wall). Whichever supply is chosen, the N_2 gas must be free of water and be supplied at a constant pressure for at least one working day. Any significant change in this pressure can cause stage drift related to the temperature change. Temperature drift will result in poor FIB-milling performance, seen as sample drift and therefore hindering the outcome of the experiment. Water is usually found in 'in-house' N_2 gas supply systems due to condensation and freezing in the pipe work, but an excessive water content can be reduced by using a commercial LN_2 water trap. Standard high-pressure (HP) cylinders of N_2 gas were used abundantly at one time for cryo-SEM, but have proved to be a constant source of contamination from water in the gas and are not advised for use in cryo-FIB-SEM work. Ultra-high-pressure (UHP) dry N_2 cylinders with 1 ppmv of water are a great improvement and are now used by many cryo-laboratories.

Water condensed and frozen in the cryo-system tubes has to be blown out by switching on the gas flow at primary working pressure for at least 10 min, before the system can be cooled down by lowering the heat exchanger into the LN_2 dewar. Failure to do this may result in a blockage in the tubes due to water freezing during operations and will need the operation to stop to dry out the tubes.

Temperature of the sample. The temperature read-out from the stage becomes less accurate when the construction of the stage + sample holder becomes more complex, that is consisting of multiple components which are either soldered, screwed or clamped against each other. In our experience a poor contact between two copper plates could easily create 10 °C loss, even though copper conducts the temperature very well. This is particularly important to consider when designing experimental stages, sample holders or carriers.

Closing a session. The cold surfaces of the cryo-stage and the anti-contaminator will accumulate large amounts of frost during the day. Once a session is finished and the equipment is warmed up, all the water vapour is released into the vacuum within a short time. As a result, safety interlocks of the microscope system may 'detect' a leakage and stop the turbo-pump, or even vent the microscope chamber. Hence it is advised not to leave the system unattended before the temperatures are above −60 °C (on both the cryo-stage and the anti-contaminator), so pressure bursts are no longer expected. More recent FIB-SEM systems have largely eliminated this problem and can be left to warm-up with automatic control.

When a system must be vented after a cryo-session, it is advised to wait for the stage and cold-trap to have reached ambient temperatures or moisture will rapidly condense onto the cold surfaces, creating difficulties later for pumping down the chamber.

Sample preparation procedures

There is no such thing as a 'typical Life Sciences sample'. The diversity and the corresponding scientific questions are enormous. When sorting the samples according to their dimensions, macromolecular complexes (viruses, proteins), membranes (individual organelles, whole cells), and even entire pieces of veins, organs and bones may be choices. Sources vary as well, and may be human or animal samples, bacteria, viruses, cultured cells or botanical samples. Depending exactly on what 'Life Sciences sample' is studied in relation to what scientific question, a specific preparation strategy needs to be applied. Choosing the correct freezing strategy is essential to prevent artefacts invalidating the results. The preparation may involve the use of chemical additives. Although a purist may want to refrain from any additives at all, it may not be feasible due to the sample nature. Freezing of water in general, and hydrated material like tissue in particular, is not trivial and was even long deemed to be impossible (Dubochet *et al.*, 1988; Dubochet, 2007). The science of freezing hydrated matter is still an active and very

relevant discipline. In Life Sciences, we can restrict ourselves to a minimum of need-to-know procedures. In other words, choosing a pragmatic approach neglects artefacts which cannot be seen by the selected imaging method. Although such negligence is common practice, including in the work of the authors, we would like to draw some attention to the fundamentals of freezing, to make sure that it is not completely overlooked. Table 1 provides an overview of sample types that have been researched by different authors along with sample support, freezing method and cryo-application.

Cryo-fixation

Water is a peculiar substance, exhibiting the most anomalous behaviour of all known liquids (Gallo *et al.*, 2016). The mechanisms of freezing water are still being debated (in particular homogeneous nucleation from supercooled water) and different routes of freezing (cooling rate, confining pressures, subsequent heating cycles) result in a variety of distinguishable phases. Considering water within a biological context (water inside and outside cells) complicates matters considerably. Water is sometimes called the 'matrix of life' and is described by controversial and poorly clarifying terminology such as 'bound', 'free', 'slow' and 'bulk-like' water (Dubochet, 2007; Szent-Györgyi, 1979; Ball, 2008; Ball, 2017). The discussion on forms of water revolves around the effect of the high concentrations of hydrophobic and hydrophilic structures present in the cells, as well as the effect of ions and their corresponding hydration shells. On average, the number of water molecules between macromolecular complexes is about four, although water in the liquid phase is supposedly already disordered at length scales exceeding two water molecules (Dubochet, 2007). Recent experimental results indicate that the majority of intracellular water behaves equivalently as 'bulk', while the fraction that behaves differently ('slow') is mainly bound to proteins, and to a lesser extent to ions and biomolecules (Tros *et al.*, 2017). In such work, the experimental distinction between 'bulk' and 'slow' is defined through the responses found by time-resolved vibrational spectroscopy and dielectric-relaxation spectroscopy.

The process of freezing cells is clear and is explained in great detail by Nobel Prize winner Jacques Dubochet (Dubochet, 2007). Casual freezing in a refrigerator allows for water molecules to form hexagonal ice crystals. Ice crystal formation causes phase segregation of insoluble molecules and creates water stress and osmotic pressure across membranes. Stress and pressure could ultimately result in ripping of the membranes which is in most cases is an unacceptable result, as it does not preserve the native state. Prevention of ice crystal formation requires ultra-fast freezing, typically with an estimated cooling rate of 10^6 °C s^{-1} or even much faster (Dubochet *et al.*, 1988; Dubochet, 2009). When water is frozen that quickly, water molecules are not able to organise themselves into a crystalline order and instantaneously standstill, including rotations. The so-called vitreous state (see 'Vitreous state' section) is obtained. Maintaining the sample at a temperature below −137 °C will preserve the vitreous state. Raising the temperature above −137 °C will induce a change into a cubic phase (Marko *et al.*, 2005; Dubochet *et al.*, 1988). It is thought that such induced phase change is not too harmful to the sample, as the change from vitreous to cubic requires only marginal displacements of the water molecules (mainly some rotations) (Dubochet, 2009). Increasing the temperature above −115 °C to −105 °C will induce another phase change into hexagonal ice (Dubochet *et al.*, 1988). Both phase changes are irreversible, meaning that a cubic or hexagonal phase will not return to vitreous status upon cooling.

Vitreous state

When water is frozen sufficiently fast, it reaches a noncrystalline, solidified state. A variety of terms are being used to describe such a state. The noncrystalline, solidified state is most often referred to as 'vitreous water' or 'vitreous ice' in the electron microscopy community. The same form of water is called amorphous solid water (ASW) in (astro)physics. At least three different phases of ASW exist: high-density amorphous (HDA) water, low-density amorphous (LDA) water and very low-density amorphous (VLDA) water. Considerations for drawing a phase diagram for ASW is still a very active research topic (Limmer & Chandler, 2014; Martelli *et al.*, 2017). The vitreous state is often considered to be equal to an amorphous state (e.g. 'amorphous solid water'. In the Life Sciences electron microscopy community, amorphous and vitreous states are interchangeable terminologies. In the physics community, these states are often distinguished from each other, based on one or multiple variations of the oxygen and hydrogen bonds (Bartels-Rausch *et al.*, 2012). Whether Life Science samples are frozen into a vitreous state, ASW or a similar form of ice/glass is not definitively known until the freezing is checked by TEM diffraction. The absence of any diffraction spots indicates that a sample is frozen well (noncrystalline). Crystalline ice could be a cubic form, which appears as certain rings in the diffractogram or a hexagonal form which appears as lattice spots. Without drawing a final conclusion in the discussion over terminology, we will continue using 'vitreous statue', with the assumption that it leaves all the biological content intact, including macromolecular complexes. The question of whether or not 'vitreous ice' is a solid or liquid phase is beyond the scope of this paper.

Freezing Life Science samples

The challenge of freezing hydrated Life Science samples into the vitreous state is limited by the thermal coefficient of

Table 1. Cryo-FIB-SEM work on Life Science samples, along with their freezing methods, found in literature.

Sample type	Carrier Support	Freezing method	Application	References
Amoebe (Dictyosteliumdiscoideum)	Membrane Carrier/TEM grid	HPF/Ethane plunge frozen	TEM prep	(Rigort *et al.*, 2010a)
Ascaris suum sperm cels	TEM grid	Ethane	TEM prep	(Zhang *et al.*, 2016)
Bacteria (Mycobacterium smegmatis)	Membrane Carrier/TEM grid	HPF/Ethane plunge frozen	TEM prep	(Rigort *et al.*, 2010a)
Bacteria inside eukaryotic host	TEM grid	Ethane	TEM prep	(Böck *et al.*, 2017, Medeiros *et al.*, 2018)
Cyanobactaria	TEM grid	Ethane	TEM prep	(Weiss *et al.*, 2019)
Chlamydomonas cells	TEM grid	Ethane	TEM prep	(Engel *et al.*, 2015)
Dictyostelium discoideum	TEM grid	Ethane	TEM prep	(Rigort *et al.*, 2012)
E. Coli	TEM grid	Ethane	TEM prep	(Zhang *et al.*, 2016)
Hela cells	TEM grid	Ethane	TEM prep	(Strunk *et al.*, 2012; Arnold *et al.*, 2016; Schaffer *et al.*, 2017; Spehner *et al.*, 2020)
Mammalian cells	TEM grid	Ethane	TEM prep	(Wang *et al.*, 2012)
Mesenchymal Stem Cells on Ti surface	Ti foil	LN2 slush plunge frozen	TEM prep	(Edwards *et al.*, 2009)
Mouse embryonic fibroblast cells	TEM grid	Ethane	TEM prep	(Zhang *et al.*, 2016)
Mouse nervous tissue	HPF carrier	HPF	FIB-SEM tomography	(Steyer *et al.*, 2019)
Neurons	TEM grid	HPF	CLEM/TEM prep	(Gorelick *et al.*, 2019; Sartori-Rupp *et al.*, 2019)
Muscle tissue (Toadfish bladder)	Membrane Carrier	HPF	TEM prep	(Hsieh *et al.*, 2014)
Onion epidermal cell wall	SEM stub	CryoMatrix + −85°C storage	FIB cross-sectioning	(Zanil *et al.*, 2015)
Osteoblast-like cells	SEM stub	LN2 plunge freeze	FIB cross-sectioning	(Lamers *et al.*, 2011)
Retinal ganglion cells (optic nerve)	HPF carrier	HPF	FIB-SEM tomography	(Schertel *et al.*, 2013)
S. Elegans	TEM grid/Cu and Al planchet	Ethane	TEM prep	(Harapinm *et al.*, 2015; Mahamid *et al.*, 2015)
SF9 insect cells	TEM grid	Ethane	TEM prep	(Zhang *et al.*, 2016)
Spores (Aspergilles Niger)	SEM stub	LN2 slush plunge frozen	Cryo-lift-out	(Rubino *et al.*, 2012)
Tobacco leaves (*Nicotiana Tabaccum*)	SEM stub	LN2 slush plunge frozen	FIB cross-sectioning	(Hayles *et al.*, 2007)
Whole sea urchin	Cu/Al planchet	HPF	FIB-SEM tomography	(Chang and Joester, 2015; Vidavsky *et al.*, 2016)
Yeast cells	TEM grid/Cu and Al planchet	HPF/ethane plunge frozen	FIB-SEM imaging/TEM prep	(Rigort *et al.*, 2010a; Hayles *et al.*, 2010; Chang and Joester, 2015; He *et al.*, 2017)
Yeast cells	tube	HPF	Cryo-TSEM	(De Winter *et al.*, 2013)
Zebrafish Larvae	Al planchet	HPF	FIB-SEM tomography	(Vidavsky *et al.*, 2016)
C. Elegans tissue	TEM grid	HPF	FIB-SEM/TEM prep/Liftout	(Schaffer *et al.*, 2019)
C. Elegans tissue	TEM grid	HPF/ethane plunge frozen	FIB-SEM/TEM prep/Liftout	(Fuest *et al.*, 2019)
Yeast	TEM grid	Ethane/propane plunge frozen	FIB-SEM/TEM prep	(Buckley *et al.*, 2020)

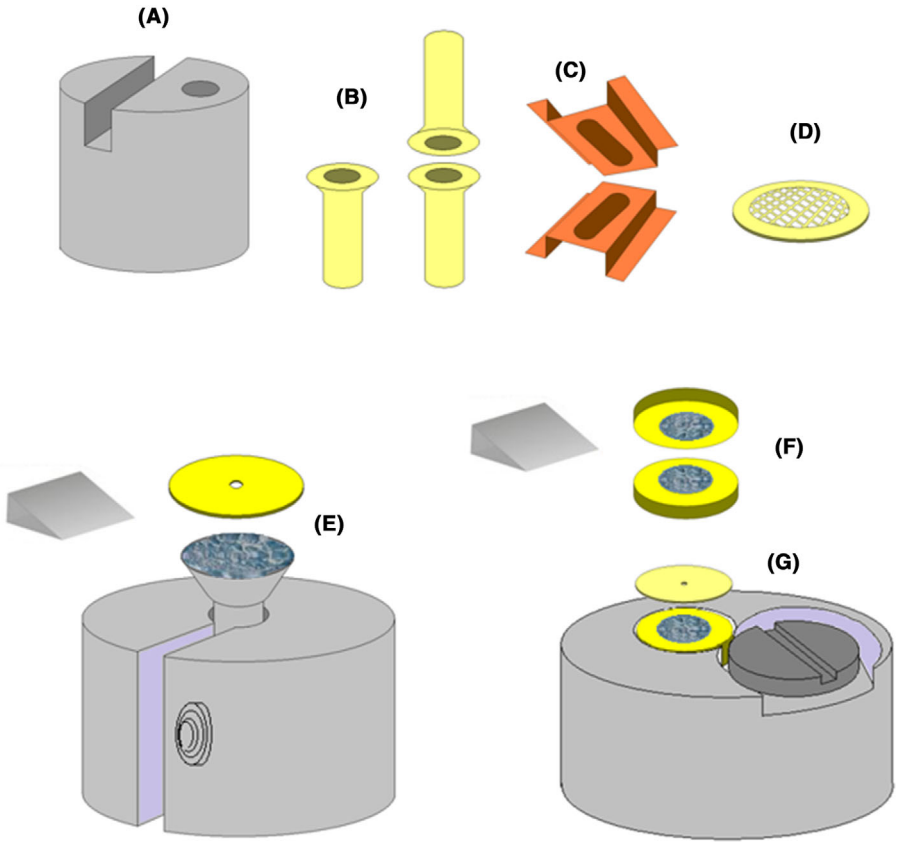

Fig. 3. Commercially available carriers: (A) 10 mm aluminium block with fracture recesses for LN_2 only. (B) Rivets for plunge freezing/fracture in suitable cryogen. (C) Planchets used the same as rivets. (D) Grids are usually associated with cryo-TEM but can be used for cross-sections if sample concentration is higher than regular TEM suspension. (E) Microstub and sapphire disc for HPF where thin layers are useful. (F), (G) Gold membrane carriers (1.5 mm diameter, 100 or 200 μm thick), two for a mid-volume fracture, one + sapphire disc for surface fracture. Bases for (E) to (G) are custom made from 10 mm half-height aluminium stubs. (All drawings not to scale.)

water itself (Gan & Jensen, 2012). As a result, the sample type and size determine the available options for preparing the samples. The vitreous state may or may not be required. Detailed molecular examination may not be the goal. In that case, a FIB cross-sectional overview obtained after plunging the sample into LN_2 slush and subsequent freeze-fracturing may be sufficient (see 'LN_2 slush' section). It is known that small details of the water phase may influence disruption in the molecular structure, potentially resulting in unreliable or false conclusions. However, most cellular or bacterial dispersions, including those in rivets or planchets, will lend themselves to plunge freezing and fracturing when using liquid ethane, propane or an ethane/propane mixture (see 'Ethane and propane' section). When dispersed onto a TEM grid, the volume to freeze is actually very small (a few micrometres thick). Hence, vitrification of isolated molecular structures can be obtained by plunge freezing TEM grids in these cryogens (Tivol *et al.*, 2008). The sample usually cannot be fractured when dispersed on a TEM grid, due to its physical nature, but otherwise can be FIB-milled to produce cross-sections. Different sample carriers are required for the three main freezing methods employed in cryo-FIB-SEM as discussed below. The most commonly used methods are depicted in (Fig. **3**).

Chemical additives. Two types of chemical additives can be used when freezing hydrated Life Science samples: a 'filler' and a 'cryo-protectant'. The ideal chemical additive is one that acts as (McDonald, 2007; Möbius *et al.*, 2010; Mielanczyk *et al.*, 2014). A filler, such as yeast paste, is used to fill up air pockets in the volume being frozen, since voids of air cause imperfect and inhomogeneous freezing. A cryo-protectant binds to water molecules, preventing ice crystallisation (Meister *et al.*, 2014). Examples of extra-cellular fillers/cryo-protectants, which are not known to enter cells or act osmotically, are dextran and hexadecane. Cells with high water content (e.g. brain tissue) may require additional intra-cellular cryo-protectants such as sucrose (Zuber *et al.*, 2005). Hexadecane is preferred for cryo-ultramicrotomy of vitreous sections, but any of the common fillers are adequate for sample pretrimming in the cryo-ultramicrotome. However, as fillers/cryo-protectants are nonconductive, their addition has been known to worsen electrical charging during FIB-milling.

Plunge freezing in LN_2 slush. The biological question to be answered primarily governs the method to be used for freezing. The need to prevent preparation artefacts that can actually affect the outcome of an experiment is a pragmatic decision. For example, demands on the freezing protocol are much higher when endeavouring to measure membrane receptor conformations rather than simply locations on a membrane. Similarly, determining invaginations versus counting vacuoles in cells. Cryo-protectants are therefore widely used to prevent some freezing artefacts when freezing bulk samples in LN_2. Rather than using liquid LN_2, it is advised to use LN_2 slush (see 'LN_2 slush' section) for this purpose. Samples are loaded into a metal carrier stub, rivet or planchet for fracturing and FIB-milling of cross-sections. Sample material close to the metal may actually be frozen into a vitreous status, whereas further into the sample crystallinity will occur.

LN_2 slush

LN_2 slush is colder than liquid LN_2. The melting temperature of N_2 is –210 °C whereas LN_2 is –196 °C. In addition, LN_2 slush prevents the so-called Leidenfrost effect (the formation of a thin gaseous layer between the warm surface and the LN_2), which strongly reduces thermal conduction (Umrath, 1974; Baker *et al.*, 2013). LN_2 slush is formed by creating a vacuum above the LN_2 for a number of minutes, depending on the volume of LN_2. Pumping can be stopped when the LN_2 solidifies; the pressure change immediately allows the N_2 to become slush.

Plunge freezing in liquid ethane/propane. Ethane and propane have lower freezing temperatures than LN_2 and therefore provide an opportunity to freeze a sample to vitreous state by plunge freezing. This is a more demanding technique but can be beneficial to the freezing of the sample. The ethane/propane will be held in a small container surrounded by a bath of LN_2 (see 'Ethane and propane' section). Although this method has been practiced widely with basic laboratory setups in the past, these days there are several commercial instruments available that will do the job safely and effectively. Sample carriers suitable for ethane/propane plunge freezing are usually rivets or planchets for fracture (see Figs. **3A–C**). TEM grids (Fig. **3D**), for cross-sectioning, can also be used if the concentration of the suspension can be increased while the total volume is kept to a minimum. The sample in general has to be smaller in volume or thinner than that for LN_2 plunge freezing if any degree of vitrification is to take place. Both the LN_2 and ethane/propane plunge-freezing methods can benefit from using clean, low-water-content LN_2 during LN_2 freezing and ethane/propane-to-LN_2 transfer. Therefore, it is important at each stage to use filtered LN_2 to prevent excessive ice contamination from absorbed water (ice) depositing on the sample. Clean LN_2 is obtained through use of Whatman filter papers (Whatman Co., Fairfield, CT, USA), to filter LN_2 immediately before use. Allowing N_2 gas to build up over the cryogen in the plunging chamber protects the cryogen surface from absorbing water from the surrounding atmosphere. The gas layer should be pumped away under vacuum before withdrawing the sample into the transfer module.

Ethane and propane

The cryogens ethane and propane can be used separately or as a mixture. In practice ethane is probably used more than propane. Reasons for this can simply be safety, since liquid propane is more volatile (flashpoint –104 °C) than liquid ethane (–130 °C). Either can be ignited if their vapour mixes with the air above the liquid, and therefore they need to be kept isolated in a container immersed in a LN_2 bath. The LN_2 offers protection from air by the N_2 gas generated from the boiling LN_2 covering the top of the ethane/propane-filled container. Ethane freezes water faster than LN_2, has no Leidenfrost effect and prevents forming cubic ice by having a greater heat capacity (melting point −188 °C compared to LN_2 at –196 °C (Ryan *et al.*, 1987).

High-pressure freezing. Cultured cells on a grid, and especially in pellets, are often too thick for vitrification in liquid ethane. Samples taken directly from tissue present a full spectrum with strongly varying properties, for example bone, skin, muscle, brain etc. These compact volumes cannot be simply plunge frozen and an advanced freezing technology is needed. High-pressure freezing (HPF) is preferred. HPF systems used by the authors are Leica EM Pact and EM Pact2 (Leica Microsystems, Vienna, Austria). Frequently in combination with HPF, chemical additives are used to prevent ice crystal formation upon freezing. Sample carriers are specific to high-pressure freezing. Frequently utilised carriers which are ideal for cryo-fracture and cross-sectioning techniques consist of micropin stubs with sapphire discs and membrane carriers (see Figs. **3E–G**).

High-pressure freezing

Ultra-fast freezing of discs of water with a thickness larger than 15 μm is made unlikely due to the poor thermal conductivity of water itself (Gan & Jensen, 2012). However, thermodynamics dictate that when increasing the ambient (confining) pressure, the melting temperature should decrease. With a confining pressure of 2000 bar, the melting temperature can be decreased to –40 °C. As a result, the jump towards –137 °C (devitrification temperature) is reduced and consequently thicknesses up to ~250 μm can be vitrified (Moor, 1987; Gan & Jensen, 2012). The sample is hit by a jet of nitrogen gas at LN_2

temperatures while exposed to the high pressure. Samples have to be mounted carefully into an HPF carrier, such as a tube or planchet. Proper closing of the carrier is crucial. Improper closing will result in the sample being blown out of its carrier. In addition, a sample should not contain any air pockets which could collapse under high pressures. One solution is the use of fillers that will fill up all voids in a sample (see 'Chemical additives' section).

Cryo-transfer

Handling and transferring a sample are a delicate exercise when considering the temperature restrictions and the forthcoming risks of contamination. It is advantageous to reduce the number of transfers as much as possible. In addition, manual handling of TEM grids and alike with tweezers under LN_2 is challenging. Therefore, specific sample holders are either manufactured along with cryo-instrumentation or custom designed to carry different grids, rods, rivets and other sample carriers, often home-made for specific applications. Sample holders submerged in LN_2 must have easy access from above. Therefore, most holders are generally clamping mechanisms, orchestrated by screws or levers. The rivet sample carrier (see Fig. **3B**) fits this type of holder and is widely used for cryo-fracturing and is also ideal for cryo-FIB-SEM work. The rivet sample carrier is usually plunge frozen either in LN_2 slush or liquid ethane/propane and can accept a variety of samples such as cryo-protected tissue samples, cell cultures and botanical sample material.

Manufacturers provide a solution for transferring a sample loaded onto a sledge-type sample holder into the microscope chamber. We assume that the protocols that come with the instrument will ensure a contaminant-free transfer of material into the cryo-FIB-SEM chamber, using the shuttle mechanism. Still, it is important to discuss the potential sources of contamination and to be able to recognise different types of contaminations (see 'Contamination' section). The sample type, mounting and scientific question will determine the follow-up, once the sample is secured in the preparation chamber. General choices to consider are cryo-fracture (see 'Cryo-fracture' section), sputter coating (see 'Sputter coating' section) or direct transfer into the cryo-FIB-SEM chamber. Before the sample is transferred into the cryo-FIB-SEM chamber, it is advised to adjust the temperature of the sample to the temperature of the stage in the microscope chamber (see 'Outside the vacuum chamber' section).

Cryo-fracture

After transferring the frozen hydrated sample to the preparation chamber fracturing of the sample may be carried out. This is important to provide a surface to work from for creating a useful cross-section for other milling needs. Some samples may not need or lend themselves to fracture, such as thin dispersions, hard bone or enamel, so the native surface will have to suffice. Fracturing the sample will create a clean surface and provide an, informative map of what features may be FIB-milled. This is a good start to targeting features of interest, whereas the native surface may obscure regions of interest, or worse, be contaminated with ice. Fracturing the sample is often associated with plunge freezing in LN_2 for cryo-SEM applications. However, contaminated HPF samples that cannot be sublimed may lend themselves to fracture as well, providing a better or surface for cryo-FIB-SEM investigation. Fracture technique is either 'open' or 'closed'. Plunge frozen samples can be 'open' (e.g. an aluminium stub or a single rivet), revealing the native material surface or 'closed' between rivets or planchets (see Figs. **3A–C**). All HPF samples are closed by means of microstubs, sapphire discs or membrane carriers (see Figs. **3E–G**). Tools used for fracture vary by manufacturer, but a sharp blade with a through-swing action generally produces the best result. The temperature of the sample at the time of fracture is vital to preserve the structure intact, without distortion. An excessive (–145 °C to –150 °C) can cause an elastic fracture such that components are pulled upon until they snap, leaving a high physical relief (see Fig. **4A**). A fracture temperature of –155 °C to –160 °C can form a regular relief structure (see Fig. **4B**) and between –160 °C and –170 °C a 'glassy', brittle fracture will occur (see Fig. **4C**), leaving little difference in topographical form on the resulting surface. These criteria may need some practice, as it is very sample dependent.

Small droplets of a cell suspension can be frozen inside rivets (Fig. **5**). It can be advantageous to roughen the flat ends of the rivets to improve the ice grip during fracture. This can be done using fine-grained sandpaper. The tube end of the lower rivet is first dipped into TissueTek© to prevent the sample liquid from running through the rivet. A small droplet of the cell suspension is pipetted onto the flat end of the rivet once it is placed in the holder. The tube end of the top rivet is also dipped in TissueTek© and is gently placed onto the lower rivet flat. Once the second rivet is in place, the entire construction can be plunged into LN_2 slush. The entire construction is loaded into a shuttle and transferred into the preparation chamber. A cryo-tool (cooled down to LN_2 temperatures) is used to quickly knock the upper rivet away, creating a fresh cryo-fractured surface.

Contamination

At different stages of making a cryo-FIB-SEM cross-section from a fracture, ice contamination can occur. Usually it is possible to recognise the type of ice contamination and therefore rectify the fault position in the procedure. The most prominent forms of ice contamination are listed here.

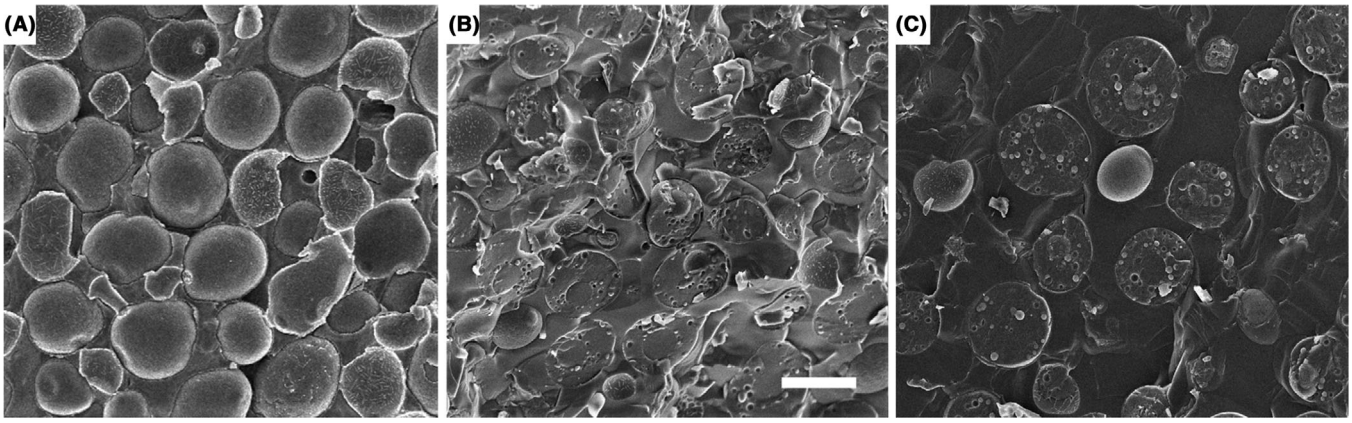

Fig. 4. Cryo-fracture: This frozen yeast culture demonstrates how temperature affects fracture. (A) Elastic fracture due to too high temperature (−150 °C, showing fracture has moved over and around cells and not through. (B) Normal fracture for SEM, some though cells and others showing fractured P2 and P3 membranes. (C) Glassy fracture, straight through most cells. Not ideal for SEM but perfect for cryo-FIB-SEM cross-sectioning. Scale bar: 5 µm.

Contamination from LN_2. LN_2 contains an amount of ice produced by absorbed water from the atmosphere at the surface. This type of contamination can be recognised by the presence of hexagonal crystals or ice balls within the mass of the contaminating ice, ranging from tens to hundreds of nanometres in diameter (Figs. **6A**, **B**). Unfortunately, the water saturation of LN_2 can dramatically increase if precautions are not adhered to during sample preparation or transfer. To prevent the buildup of ice, all LN_2 used in preparation and transfer should be filtered as mentioned above and poured into clean and dry dewars that are capped (but not closed air tight). When refreshing LN_2 in the equipment, filtering yet again from the working dewars is recommended. Storage of cryo-samples placed in and taken out of storage dewars on a frequent basis will give rise to contaminated LN_2. Just replenishment without filtering of LN_2 into these containers gives rise to the LN_2 ice contamination. This type of contamination is restricted to the original surface prior to milling and may not be realised until viewed in the cryo-FIB-SEM, by which time the sample could have been sputter coated with metal. The contamination is usually large and irregular (Figs. **6A**, **B**). Sublimation for nonvitreous samples may be an option, but this type of contamination is robust in nature and therefore could easily be underestimated. It would take significant time to mill away and may inadvertently affect the true surface in the process or decimating any metal coating present. The option of returning the sample to the cryo-preparation station for fracturing a vitreous or nonvitreous sample is preferred by the authors. This method of recovery is quick and safe. In the case of a vitrified sample with a specific site of interest that could be lost in fracture, gentle ion milling would be the only option instead of replacing the sample.

On a practical note, forceps should be hand-warmed and dry before entering them into LN_2, in particular when reusing forceps that have been previously immersed in LN_2. Having multiple forceps available to use consecutively could come in handy when speed is important. As a rule of thumb, the portion of the forceps initially immersed in LN_2 will have cooled

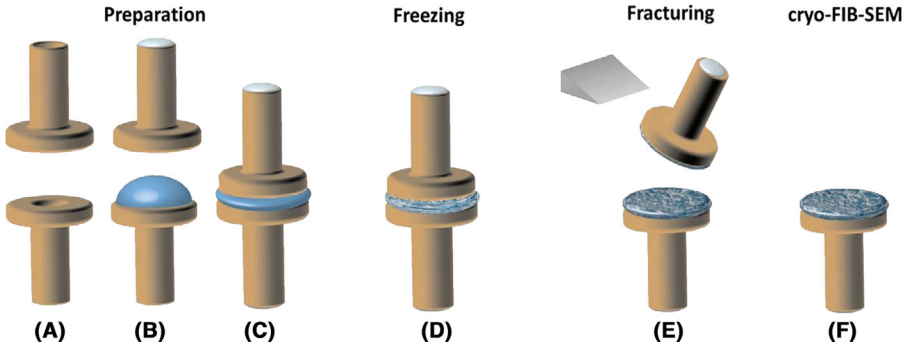

Fig. 5. Creating a cryo-fracture surface with two rivets. (A) The flat surfaces of both rivets are roughened with sandpaper to increase the contact surface between the rivets and the sample. (B) The rivet-ends are closed with TissueTek™ to prevent leakage. A droplet of sample is placed on the lower rivet. (C) The second rivet is carefully placed on top. (D) The ensemble is frozen by lowering it vertically into LN_2 slush or liquid ethane/propane. (E) A precooled knife knocks off the top rivet when in the transfer station, creating a fracture surface. (F) The fracture surface is sputter coated with a metal to prevent electrical charging. It is now ready for transfer into the cryo-FIB-SEM.

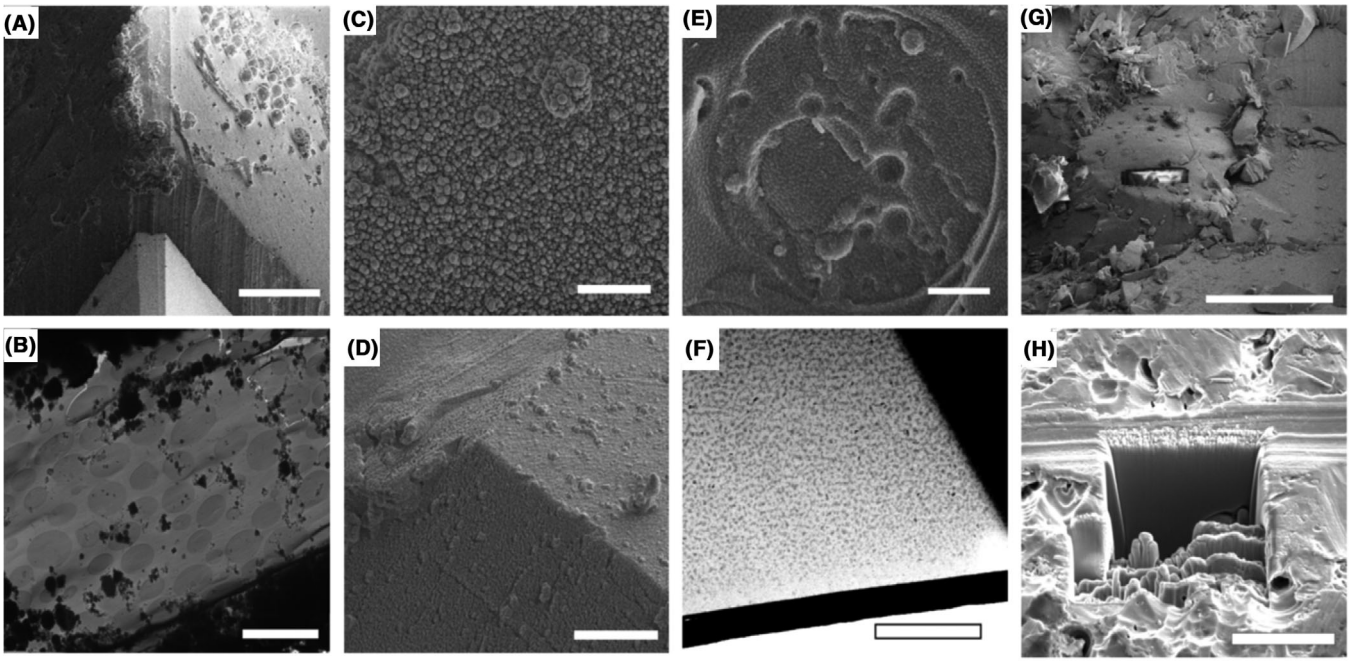

Fig. 6. Contamination types: (A), (B) Examples of LN_2 born ice crystals deposited on the surface. (C), (D) Ice crystals condensed on the surface from air exposure. (E), (F) Temperature differential contamination "orange peel" caused by a warm surface in the close vicinity of the sample. (G) Debris from the fracture process. (H) Redeposition from the ion beam milling process. The redeposition is recognisable from the sides of the cross-section which become increasingly 'bulging' in front of the cross-section during prolonged milling. Scale bars: (A) 50 μm, (B) 10 μm, (C) 5 μm, (D) 50 μm, (E) 2 μm, (F) 2 μm, (G) 100 μm and (H) 20 μm.

down sufficiently when the bubbling of the LN_2 has stopped. Otherwise, heat from the forceps can be transferred to the sample and induce a phase transformation.

Contamination from the atmosphere. Ice can build up very quickly on the surface of the frozen sample if the sample is exposed to the atmosphere. Water from the atmosphere condenses onto the surface and immediately freezes producing a granular ('cauliflower') pattern over the entire surface (Figs. **6C**, **D**). This type of ice can contaminate samples during any transfer that accidently is exposed to atmosphere, most notably during transfer into and out of the cryo-preparation chamber. Contamination is particularly undesirable on vitrified samples that are not to be fractured or sublimated. The ice contamination can create curtaining during milling. Nonvitrified samples that suffer from this contamination can be sublimed or cryo-fractured prior to sputter coating to remove the ice.

Temperature differential contamination. The sample must not come into close proximity to a warm body (e.g. the electron pole piece) while the sample is in the vacuum chamber. Water absorbed onto a warm surface is likely to be released onto any colder surface, including the sample surface. With regards to TEM samples, this is sometimes referred to as 'orange-peel'. In the cryo-FIB-SEM it will start with very small ice growth sites and may escalate to an ice labyrinth covering all surfaces (Figs. **6E**, **F**). This can be prevented in two ways: (1) keep the sample clear of warm surfaces or shield the warm surfaces with anti-contaminator plates and (2) make sure that the anti-contaminator is at least 20 °C cooler than the sample temperature (see 'Outside the vacuum chamber' section).

Fracture and FIB-milling contamination. The fracture process is a severe attack on the sample. Pieces of the sample break and shatter away from the point of impact. Unfortunately, some of the debris may remain on the newly produced surface (Fig. **6G**). The debris may become part of the surface, or worse, become statically charged and remain attracted to the new cross-section one has just made. Immediately after fracture, releasing the sample holder and giving it a tap on the cryo-preparation table will usually remove any loose debris. The contamination is usually seen as angular pieces of ice of varying size. If charged, they appear brighter than the surrounding area.

Redepositing of FIB-milled material (Fig. **6H**) can be a problem for making cross-sections if some conditions are not ideal at the time of milling. The most common issue is the use of an excessive FIB current or the production of high-aspect-ratio trenches. In a few circumstances, the sample itself can be the problem. For example, fat particles are generally difficult to mill and may cause an irregular milling pattern leading to redeposited material by deflecting ions… The rapid release of large amounts of material under these circumstances is

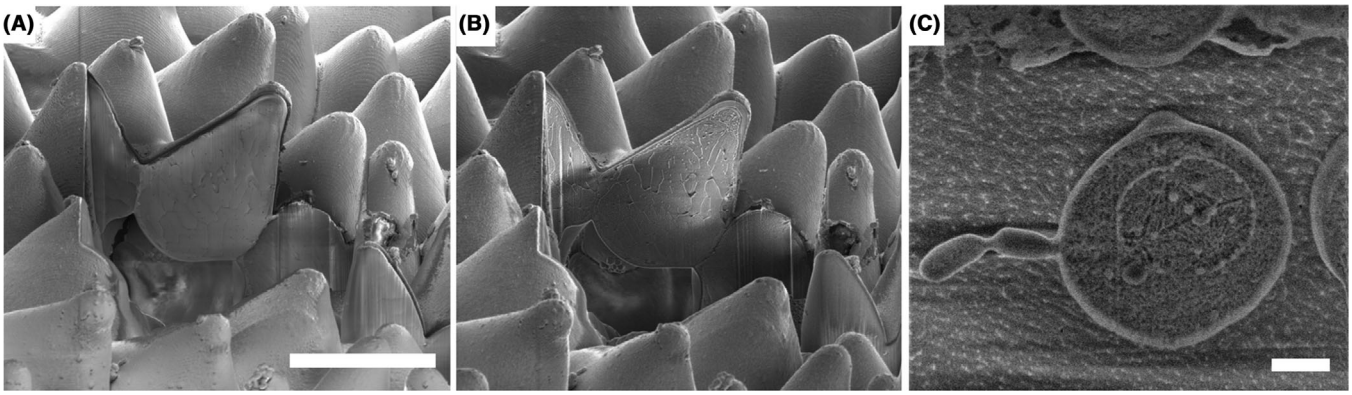

Fig. 7. Sublimation: Tobacco leaf structure. (A) After FIB-milling showing low contrast, (B) after sublimation, removing minimal water to give contrast. (C) Yeast cell after sublimation displaying Mitosis. Scale bars: (A) and (B) 30 μm and (C) 1 μm.

collected by the surrounding cold sides of the cross-section trench. Redeposition can very quickly build up on the sides of the trench not presently being milled, closing the trench and reducing visibility of the milled surface area.

Nano-ice contamination. Over a timespan of many hours, residual water vapour left in the microscope chamber forms an amorphous layer of a few nanometre on top of the sample. This becomes particularly noticeable when conducting long runs of electron backscatter diffraction (EBSD) (Weikusat *et al.*, 2011) or performing TEM prep (Schaffer *et al.*, 2017). Locally this can be irradiated away for a short time with a gentle ion beam, but it can become particularly repetitive as the session progresses if no anti-contamination device (ACD) is in operation.

Reducing the residual water vapour in the microscope requires either long pumping times (days), without opening the chamber or by using an ACD attached to the chamber. The latter will extract residual water found in the chamber and in a shorter time (overnight). An ACD is most effective in use during long cryo-sessions. In case devitrification is not an issue and with an ACD in place one could raise the stage temperature to approximately –120 °C in an attempt to sublime the contaminating ice (see 'Sublimation' section). Without an ACD in operation, the water released from the sample would normally remain in the vacuum chamber and eventually condense back to the cryo-components, including the sample (Weikusat *et al.*, 2011; Schaffer *et al.*, 2017). If no ACD is present, all sublimation cycles should be performed in the cryo-preparation chamber so that sublimed water vapour does not enter the FIB-SEM microscope chamber.

Sublimation strategy

Ice exposed to vacuum will undergo a phase change from solidified directly to gas; a phase change called sublimation. The rate of sublimation is determined by the temperature of the ice and the pressure. Sufficiently low temperatures (lower than –120 °C) in a typical SEM vacuum chamber prevent the sample from subliming at a rate that is noticeable during a day's work (see 'Sublimation' section). Sublimation can be used to one's advantage. Sublimation (i.e. freeze drying) removes the water from in between cells exposed to the chamber vacuum. Cells can be opened either due to freeze fracturing or FIB-milling. In either case, also water being exposed to the chamber vacuum from within open cells is removed by sublimation. Cellular components become visible as structures on the surface (Walther, 2003). FIB-milled cross-sections benefit from sublimation in particular, as the cross-sections are generally very smooth and hence show very little contrast, except from charging ('SEM contrast from sublimation' section). Sublimation can be done in the microscope (*in situ*) (see Figs. **7A**, **B**) or outside the microscope (*ex situ*) (see Fig. **7C**). The main challenge is to prevent overdoing the sublimation, since drawing out too much water leaves the membrane structures vulnerable to damage by either the FIB or SEM beams. Sublimation can be performed in the cryo-FIB-SEM chamber only if the cold-trap is regulated at a 20 °C difference lower than the sample's lowest temperature. In addition, an on-chamber cryo-pump is useful to keep the chamber free of any water vapour created by sublimation. The advantage of *ex situ* sublimation is that it helps reduce the level of water vapour otherwise accumulating in the microscope chamber. The timing for sublimation varies sample, so monitoring the sublimation process within the cryo-FIB-SEM is a key advantage of *in situ* sublimation.

Sublimation

Control of the sublimation process is limited. First the temperature of the cryo-stage is increased to a value between –100 °C (very slow sublimation) and –85 °C (very rapid sublimation). While the heating element of the stage is warming up, the bulk of the stage is heating up at a slower rate. Furthermore, the sample will heat up at an even slower rate. As a result, the temperature at the surface of the sample (and any FIB-milled cross-sections) will reach the

sublimation conditions only after a couple of minutes. Depending on the pressure-temperature conditions, a sublimation time of 30 s to 2 min is generally sufficient. However, cooling down the sample and the stage also takes time. Hence, sublimating a predetermined thickness away (e.g. 25 nm) is practically impossible. It requires experience of the operator with the equipment and the sample type to obtain the desired results. Nevertheless, sublimation is a well-known technique that is often successfully applied to obtain new insights into frozen-hydrated samples.

Sputter coating. Most hydrated samples are poor electrical conductors, which can be troublesome for cryo-FIB-SEM operations. The electrical conductivity can be improved by sputter coating a thin metal layer (~5–10 nm, typically Pt, Pt/Pd or Au/Pd) across the entire sample. Since a layer is formed across the entire surface, any major sublimation cycle has to be carried out prior to sputter coating. If sublimation has to be performed on a contaminated metal-coated sample, extra care should be taken not to remove water molecules from below the metal layer.

Safe transfer into the microscope chamber. The temperature of the sample in the preparation chamber after fracture, sublimation and sputter coating, is adjusted to that of the cryo-stage in the microscope chamber once the sample is ready for cryo-FIB-SEM investigations. The rule of thumb is to movie a sample from warm to cold, preventing ice contamination on the sample on arrival in the cryo-stage. A crucial safety aspect when transferring samples into the microscope chamber is to close the valves to the electron beam and the ion beam (done automatically in most recent systems). In case of a mishap, a sudden gust of air may be let into the microscope chamber. Since such an event is likely to stop the cryo-session for the day, and closing the valves to the beams prevents significant damage to the electron and ion source, which would require considerably more time to recover.

FIB-SEM operations

It is advised to use 'subtle' e-beam scan conditions (e.g. 2 kV, <0.1 nA, fast scan rate) when exploring a fresh sample. Hydrated material is vulnerable to electron and ion beam radiation damage. The electrical conductivity is still poor, even after sputter-coating. The sputter-coated layer is generally thin and easily removed by the FIB. A cautious approach is required with a new sample. High kilovolts and currents (SEM, FIB, or both) will cause severe charging effects, which may cause image distortions and prolonged drifting. The FIB ion beam current must be reduced (e.g. to ~10 pA), since if left high the sample can be devastated. In general, neither of the beams should be left scanning, unless it is necessary to generate an image or mill a feature. Setting up the eucentric point of the FIB and SEM beams (see 'Cryo-FIB-SEM' section) can be done according to the standard routines corresponding to the specific microscope being used, with the exception of stage rotation. When ready, and when the area of interest is found, one can decide to cover the sample surface by using *in situ* Pt deposition, similar to that for room temperature samples. The Pt layer protects the surface from the ion beam, while it improves the finish of the cross-section due to better smoothness of the top surface. The procedure has been adapted for cryo-applications and is described in detail by Hayles *et al.* (2007) (see 'Sample protection' section) (Hayles *et al.*, 2007).

Sample protection

In situ Pt deposition makes use of a needle valve that releases an organometallic precursor gas close to the surface of the sample. At room temperature, the inert gas diffuses across the surface. The gas molecules are dissociated by the ion beam into volatile components and adsorbed (metallic) components. The latter forms the protective layer. Electron beam induced deposition is also possible in principle, but it is very slow, and to the author's knowledge has not been used under cryo-conditions.

Under cryo-conditions, the precursor gas immediately freezes onto the sample surface, instead of simply diffusing across it. Hence a small amount of precursor and a brief flow is required. Restricting the dosage by controlling the needle valve prevents growing massive mountains on top of the region of interest. The temperature of the crucible is set to approximately 28 °C for 'cryo' use (see 'Crucible temperature' section). Moreover, the stage is lowered approximately 1 mm lower than its normal operating position. Lowering the stage will spread the gas flux across a wider area.

The needle valve is opened manually for ~3–5 s only, since the deposition layer grows rapidly. The growth process can be monitored live with the electron beam. It is advantageous to increase the temperature of the sample to –125 °C to improve the homogeneity of the deposition (less gas trapped inside the deposited layer). However, increasing the temperature can only be done when the vitreous state is not required.

The needle can be retracted once the valve is closed, and the stage can be brought back up to its normal operating position. At this point, the precursor molecules would be adsorbed to the surface, but not yet dissociated. This is done by moderate irradiation with the ion beam (typically 30 kV, 1 nA). Continuous scanning by the ion beam will gradually dissociate the precursor molecules, a process called planerising. The dissociation can be monitored live using the electron beam, reflected in a very bright image due to the release of secondary electrons from the interaction between the primary electrons and the escaping volatile gas components. Once the electron beam image turns darker, the

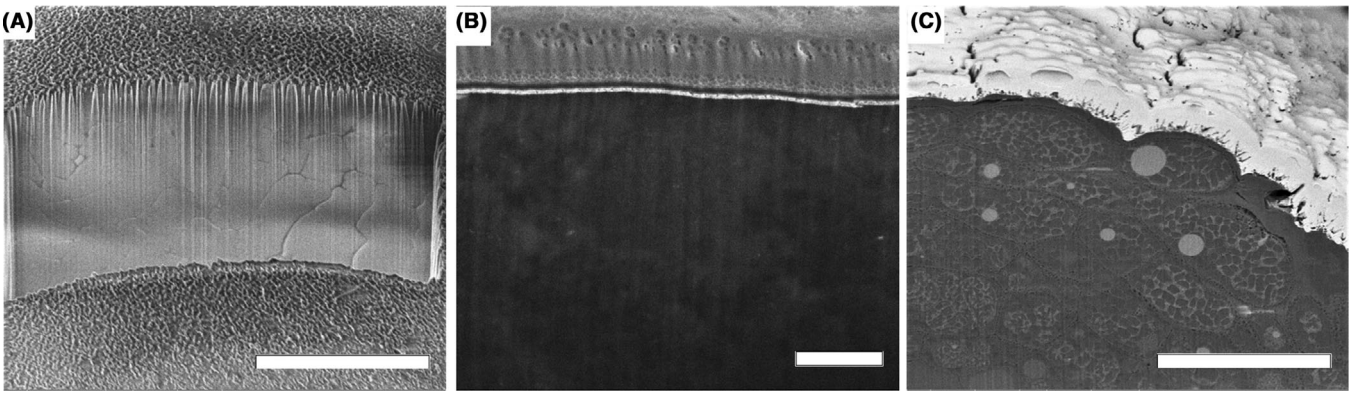

Fig. 8. Curtaining and protection: (A) Surface roughness causing severe curtaining. (B) Cryo-sample showing Au/Pd sputter coating (bright line), followed by contaminating ice (dark line) from transfer, influencing the protection layer by insufficient release of gas on planerising. In turn the gas voids create curtaining. (C) An uneven surface (Mildew spore pod), covered by protective deposition, to improve and reduce the chance of curtaining. Scale bar for (A) 10 μm, (B) 2 μm and (C) 10 μm.

dissociation process has finished and the protection layer, now smoothed, is ready to be used.

FIB-milling

FIB-milling of a frozen hydrated sample under 'cryo' conditions is similar to FIB-milling of any other solid, although the sputter yield is unusually high (Marko *et al.*, 2005, Fu *et al.*, 2008). Scan strategies for efficient milling vary by manufacturer, but standard FIB-milling procedures can be followed for making cross-sections, although relatively low currents will already suffice for large cross-sections. In general, a higher current (30 kV, >1 nA) is used to make a wide trench, followed by a lower current to polish the cross-section. It is important to realise the vulnerability of the sample, hence it is advised to check and improve the focus and astigmatism correction adjacent to the area of interest.

Curtaining. A well-known challenge in FIB-milling is an artefact called curtaining. Vertical grooves or striations along the direction of the FIB distort the image of the features present in the cross-section. Curtaining is caused by local variations in ion scattering (e.g. surface roughness) along the surface of the sample as the cross-section is milled. The ion beam will mill a wider track after leaving a strongly scattering component, a starting point for a streak in the cross-section. In solid samples with a constant scattering property (such as one with a smooth and uniform surface) curtaining is rarely encountered (see Fig. **8A**). Milling frozen cells that contain dense fat bodies often results in local curtaining. The ion beam widens due to scattering, resulting in a vertical trench along the cross-section. Because the sputter yield in hydrated samples is so high, curtaining is likely to occur between high-density pockets and highly hydrated phases. Ice contamination present on the surface after sputter coating should be avoided. The contamination will be trapped by the protection layer and can cause poor deposition (gas pockets) thus inciting curtaining (see Fig. **8B**). Curtaining caused by surface roughness can be prevented by smoothing the surface with a layer of Pt deposition (see Fig. **8C**) (see 'Sample protection' section).

FIB-induced heating effect. A reoccurring question is the potential for FIB-induced heating and related damage to cryo-samples. FIB-induced heating has long been a concern, and not exclusively for cryo-applications; for example polymers and freeze-dried cellular materials are also potentially vulnerable samples (Volkert and Minor, 2007; Ishitani and Kaga, 1995; Ishitani and Yaguchi, 1996; Bassim *et al.*, 2012; Wolff *et al.*, 2018). A crucial finding is made by TEM diffraction measurements of FIB-milled cryo-sections, revealing that the FIB-milling process did not induce a phase change from vitreous to crystalline (Marko *et al.*, 2005). Although the experimental evidence is clear, theory predicts a considerable heat pulse, but damage is only to be expected very close to the milled surface. Observations of surface-damage layers confirm a typical thickness of only a few nm for low-kV FIB-milling (Schaffer *et al.*, 2012).

Effective milling is a cumulative effect and hence the accumulation of energy (i.e. phonons and heat) is considered, but accumulation occurs only if a succeeding ion enters the same space before the energy of the preceding ion has been dissipated.

Ion-beam currents in FIB-SEM instruments range from 60 nA to 1 pA. The ion-beam profile is assumed to be Gaussian (Ali and Hung, 2006; Shorubalko *et al.*, 2017). The width of the beam (i.e. spot size) is traditionally defined by the full-width-half-maximum (FWHM) or the standard deviation (SD). This is strongly dependent on the selected current and varies from 10 nm (at 10 pA current) to possibly thousands of nanometres (at 60 nA current).

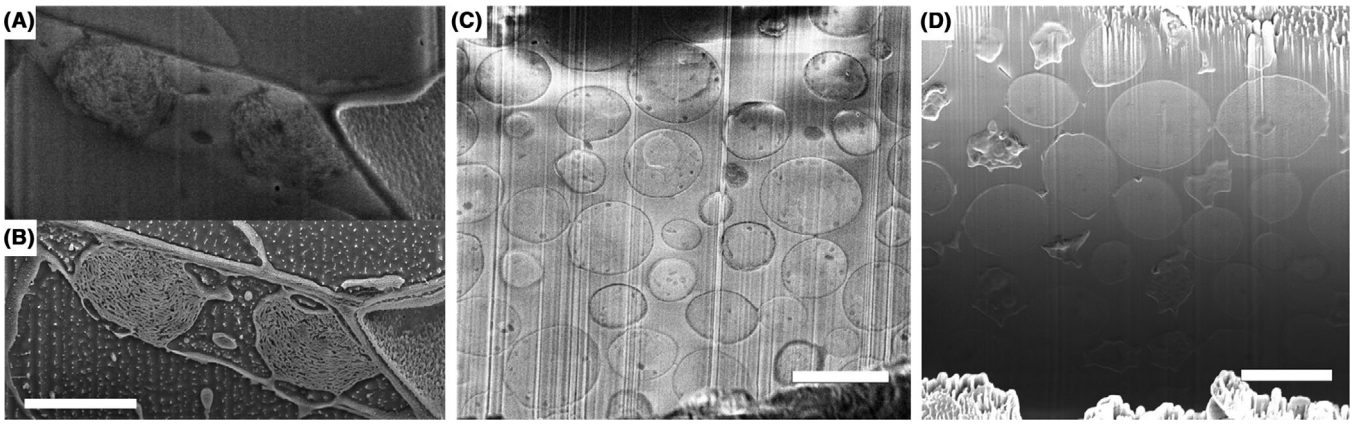

Fig. 9. Contrast: (A) After FIB-milling. (B) Creating contrast by sublimation. (C) Surface charging at 3 kV (more contrast, more charge effect). (D) Subsurface charging at 5 kV (less visual charge, more depth effect). The latter two images show the influence of different SEM beam energies and how the use and reproducibility can be a challenge. Scale bars: (A), (B) 3 μm, (C) and (D) 5 μm.

The spatial and temporal spreading of the ions across the spot size reduces the probability that a local accumulation of energy could occur. A detailed discussion of a stochastic approach towards ion-beam heating is beyond the scope of this paper.

SEM imaging

SEM imaging of cryo-FIB-SEM milled cross-sections in a frozen bulk sample presents a challenge, as the content of Life Science samples in general provides very little basis for contrast. Cells embedded in a resin are usually heavily stained with heavy metals, providing strong contrast, especially in BSE imaging mode (De Winter *et al.*, 2009), but poststaining frozen-hydrated samples is not possible. Two methods are known to visibility of cellular structures: sublimation and charging.

SEM contrast from sublimation. The principles and practical aspects of sublimation have been discussed in 'Sublimation strategy' section. A particular disadvantage of sublimation is loss of the vitreous. Not only the sample surface is warmed up, but the entire sample is heated, since the heat comes from the stage. In defence of sublimation practices, one can say that the effects of devitrification are below the resolving power of SEMs. This argument does not hold when samples are prepared by cryo-FIB-SEM for further investigations in a cryo-TEM.

An example of what sublimation can produce, is shown in Figures **9**(**A**) and (**B**). In general, FIB cross-sectioning in combination with sublimation is used for single cross-sections only. Serial-sectioning combined with sublimation cycles is deemed unfeasible due to the poor control over the sublimation process.

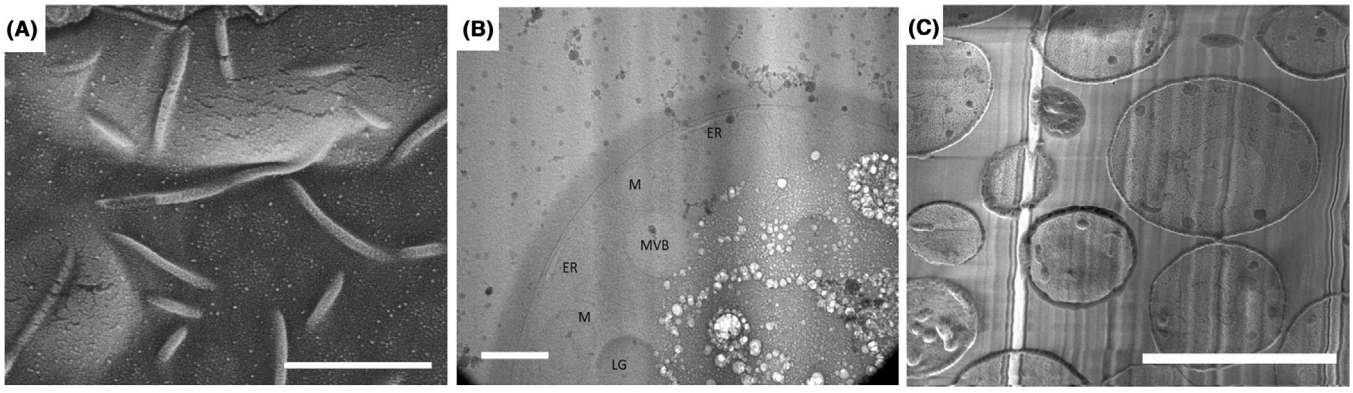

Fig. 10. Localised beam damage: (A) cryo-FIB-SEM E-beam damage after fracture and before milling of P2 inner membrane (Yeast cell) seen as swelling and splitting. Invaginations and particle arrays are visible. (B) TEM image of a cryo-FIB-SEM prepared lamella of yeast cells, demonstrating 'bubbling' of cellular component due to excessive exposure to the TEM E-beam. The FIB lamella has a thickness of 300 nm and although damaged, typical structures of *S. cerevisiae* are seen; multivesicular bodies (MVB), mitochondria (M), lipid granules (LG) and cortical endoplasmic reticulum (ER) are clearly visible. (C) Swelling of the cell walls due to over E-beam scanning. Scale bars: (A) 500 nm, (B) 500 nm, (C) 5 μm.

SEM contrast by charging. An alternative imaging strategy utilises charging phenomena present in the surface and subsurface of the FIB-milled section and has been shown recently. Life Science samples are generally poor electrical conductors and as a result, the sample charges. Charging occurs at the active milling site and is visualised in the SE imaging mod. With optimised scanning conditions of both ion and electron beam, it becomes possible to generate high-resolution images with clear details of membrane structures within. The exact image formation mechanism is complex and not entirely understood and authors have long considered such images to be with 'charging-artefact'. We believe the technique is at an early stage in development and somewhat problematic in terms of ease of use and reproducibility (see Figs. **9C** and **D**). As a 3D imaging strategy for macro and microstructures it is suited for serial-section data acquisition and 3D reconstruction, characterised by Kuba *et al*. (2020) and Schertel *et al*. (2013).

Electron beam effects. Hydrated samples are very vulnerable to the electron beam. Hydrolysis and knock-on damage occur during radiation, even when using a low-kilovolt electron beam. The sputter yield (an equivalent weight of a H_2O molecule per incoming electron) of pure water ice is found to be 1.5–0.65 for electron energies of 1–3 keV respectively (Galli *et al.*, 2018). The sputtered species consist of H^+, H_2, O^-, $O_{,2}$, HO, H_2O, H_3O and others (Galli *et al.*, 2018). When water is expelled from the sample, membrane-bound structures can swell. For example, the interaction between the incoming electrons and pure water is relatively little compared to the interaction with a membrane. As a result, relatively large amounts of energy are deposited in the direct vicinity of membranes, sometimes seen in the cryo-FIB-SEM as swelling and splitting of the membrane or swelling of the cell walls (see Figs. **10A** and **C**), or in the cryo-TEM image as bubbling (Fig. **10B**). Such damaged material can be removed by milling away or fracturing more material from the parent sample, but with the potential of completely losing a particular feature. The best solution is prevention by using the lowest electron beam current possible. In addition, focusing should be done on a part of the sample that does not contain information of interest. The latest FIB-SEM detectors have improved considerably in terms of signal-to-noise ratio, which allows for use of much lower beam currents for an acceptable image.

Conclusion/outlook

The importance and relevance of cryogenic observations of hydrated samples in Life Sciences has been underlined by granting pioneers in the field of cryo-electron microscopy a Nobel Prize. This success is the result of the combined efforts and determination of skilled mechanical and electrical engineers, physicists and biologists, facilitated by the development of high-end cryo-FIB-SEM and cryo-TEM instruments. Various practical approaches are proven to work, as discussed elsewhere in this special issue (Kuba *et al*., 2020; Parmenter, 2020; De Winter *et al*., 2020). Moreover, new biological insights have been obtained with the new techniques. As a result, many laboratories around the world have started to adopt cryo-FIB-SEM methods. Practical improvements in the workflow are needed to facilitate ease of use, speed and overall success rate before such methods become 'mature'. As new results emerge, fundamental topics are increasingly being challenged. New developments, such as application of cryo-transmission scanning electron microscopy (cryo-TSEM) add a new SEM imaging modality for single or multiple *in situ* FIB-milled thin lamella (De Winter *et al*., 2013). Another application with interesting potential is cryo-FIB-SEM serial-section data acquisition and 3D reconstruction (Kuba *et al*., 2020; Schertel *et al*., 2013; Spehner *et al*., 2020). A third example is 'cryo-CLEM' (Correlative Light and Electron Microscopy). While cryo-CLEM may take several forms, recent interesting results have been obtained by the refined application of automated FIB-milling of cells labelled for correlative light microscopy combined with cryo-lift-out for subsequent tomography in the cryo-TEM (Rigort *et al*., 2010b; Medeiros *et al*., 2018a; Sartori-Rupp *et al*., 2019; Gorelick *et al*., 2019). The cryo-lift-out technique itself is improving with encouraging interest, and already plays an important role in cryo-TEM investigations (Kuba *et al*., 2020; Wolff *et al*., 2019).

In conclusion, we hope to have convinced researchers new in the field of cryo-FIB-SEM that the technique is reasonably user-friendly and can be mastered with some practice and with the tips given. We have brought together most of the detailed knowledge, which is sometimes hidden 'between the lines' of papers discussing cryo-FIB-SEM results. It is our hope that this paper functions as a common basis for venturing into other advanced disciplines relevant to cryo-FIB-SEM research.

Acknowledgement

Dr, K.C. Findlay of the John Innes Centre, Norwich, UK is gratefully acknowledged for providing the specimen for Figures **7**(**A**) and (**B**).

References

Ali, M.Y. & Hung, N.P. (2006) Surface roughness of sputtered silicon. II. Model verification. *Mater. Manufact. Process.* **16**, 315–329.

Arnold, J., Mahamid, J., Lucic, V. *et al*. (2016) Site-specific cryo-focused ion beam sample preparation guided by 3D correlative microscopy. *Biophys. J.* **110**, 860–869.

Baker, M.J., Denton, T.T. & Herr, C. (2013) An explanation for why it is difficult to form slush nitrogen from liquid nitrogen used previously for this purpose. *Cryobiol.* **66**, 43–46.

Ball, P. (2008) Water as an active constituent in cell biology. *Chem. Rev.* **108**, 74–108.

Ball, P. (2017) Water is an active matrix of life for cell and molecular biology. *PNAS* **114**, 13327–13335.

Bartels-Rausch, T., Bergeron, V., Cartwright, J.H.E. *et al.* (2012). Ice structures, patterns, and processes: a view across the icefields. *Rev. Modern Phys.* **84**(2), 885–944.

Bassim, N.D., De Gregorio, B.T., Kilcoyne, A.L.D., Scott, K., Chou, T., Wirick, S., Cody, G. & Stroud, R.M. (2012) Minimizing damage during FIB sample preparation of soft materials. *J. Microsc.* **245**, 288–301.

Böck, D., Medeiros, J.M., Tsao, H.-F., Penz, T., Weiss, G.L., Aistleitner, K., Horn, M. & Pilhofer, M. (2017) In situ architecture, function, and evolution of a contractile injection system. *Science* **357**, 713–717.

Buckley, G., Gervinskas, G., Taveneau, C., Venugopal, H., Whisstock, J.C. & de Marco, A. (2020) Automated cryo-lamella preparation for high-throughput in-situ structural biology. *J. Struct. Biol.* **210**, 2.

Chang, I.Y.T. & Joester, D. (2015) Cryo-planing of frozen-hydrated samples using cryo triple ion gun milling (CryoTIGM^{TM}) *J. Struct. Biol.* **192**, 569–579.

De Winter D.A.M., Hsieh C., Marko M. & Hayles M.F. (2020) Cryo-FIB preparation of whole cells and tissue for cryo-TEM: use of high-pressure frozen specimens in tubes and planchets. *J. Microsc.* This issue.

De Winter, D.A.M., Mesman, R.J., Hayles, M.F., Schneijdenberg, C.T.W.M., Mathisen, C. & Post, J.A. (2013) In-situ integrity control of frozen-hydrated, vitreous lamellas prepared by the cryo-focused ion beam-scanning electron microscope. *J. Struct. Biol.* **183**, 11–18.

De Winter, D.A.M., Schneijdenberg, C.T.W.M., Lebbink, M.N., Lich, B., Verkleij, A.J., Drury, M.R. & Humbel, B.M. (2009) Tomography of insulating biological and geological materials using focused ion beam (FIB) sectioning and low-kV BSE imaging. *J. Microsc.* **233**, 372–383.

Dubochet, J. (2007) The physics of rapid cooling and its implications for cryoimmobilization of cells. *Meth. Cell Biol.* **79**, 7–21.

Dubochet, J. (2009) The physics of rapid cooling and its implications for cryoimmobilization of cells. *Vitreous water. Handbook of Cryo-Preparation Methods for Electron Microscopy* (ed. by A. Cavalier, D. Spehner & B.M. Humber), pp. 7–21. CRC Press, ISBN 978-0-84937227-8.

Dubochet, J., Adrian, M., Chang, J.-J., Homo, J.-C., Lepault, J., McDowall, A.W. & Schultz, P. (1988) Cryo-electron microscopy of vitrified specimens. *Quarter. Rev. Biophys.* **21**, 129–228.

Edwards, H.K., Fay, M.W., Anderson, S.I., Scotchford, C.A., Grant, D.M. & Brown, P.D. (2009) An appraisal of ultramicroscopy, FIBSEM and cryogenic FIBSEM techniques for the sectioning of biological cells in titanium substrates for TEM investigation. *J. Microsc.* **234**, 16–25.

Engel, B.D., Schaffer, M., Albert, S., Asano, S., Plitzko, J.M. & Baumeister, W. (2015) In situ structural analysis of Golgi intracisternal protein arrays. *PNAS* **112**, 11264–11269.

Fu, J., Joshi, S.B. & Catchmark, J. (2008) Sputtering rate of micromilling on water ice with focused ion beam in a cryogenic environment. *J. Vac. Sci. Technol. A* **26**, 422–429.

Fuest, M., Schaffer, M., Nocera, G.M. *et al.* (2019) *In situ* microfluidic cryofixation for cryo-focused-ion-beam milling and cryo-electron tomography. *Sci. Rep.* **9**, 19133.

Galli, A., Vorburger, A., Wurz, P. *et al.* (2018) 0.2 to 10 keV electrons interacting with water ice: radiolysis, sputtering, and sublimation. *Planet. Space Sci.* **155**, 91–98.

Gallo, P., Amann-Winkel, K., Angell, C.A. *et al.* (2016) Water: a tale of two liquids. *Chem. Rev.* **116**, 7463–7500.

Gan, L. & Jensen, G.J. (2012) Electron tomography of cells. *Q. Rev. Biophys.* **45**, 27–56.

Gorelick, S., Buckley, G., Gervinskas, G. *et al.* (2019) PIE-scope, integrated cryo-correlative light and FIB/SEM microscopy. *eLife* **2019**, 8e45919.

Harapinm J., Börmel, M., Sapra, K.T., Brunner, D., Kaech, A. & Medalia, O. (2015) Structural analysis of multicellular organisms with cryo-electron tomography. *Nat. Meth.* **12**, 634–636.

Hayles, M.F., De Winter, D.A.M., Schneijdenberg, C.T.W.M. *et al.* (2010) The making of frozen-hydrated, vitreous lamellas from cells for cryo-electron microscopy. *J. Struct. Biol.* **172**, 180–190.

Hayles, M.F., Stokes, D.J., Phifer, D. & Findlay, K.C. (2007) A technique for improved focused ion beam milling of cryo-prepared life science specimens. *J. Microsc.* **226**, 263–269.

He, J., Hsieh, C., Wu, Y., Schmelzer, T., Wang, P., Lin, Y., Marko, M. & Sui, H. (2017) CryoFIB specimen preparation for use in a cartridge-type cryo-TEM. *J. Struct. Biol.* **199**, 114–119.

Hsieh, C., Schmelzer, T., Kishchenko, G., Wagenknecht, T. & Marko, M. (2014) Practical workflow for cryo-focused-ion-beam milling of tissues and cells for cryo-TEM tomography. *J. Struct. Biol.* **185**, 32–41.

Ishitani, T. & Kaga, H. (1995) Calculation of local temperature rise in focused-ion-beam sample preparation. *J. Electron Microsc.* **44**, 331–336.

Ishitani, T. & Yaguchi, T. (1996) Cross-sectional sample preparation by focused ion beam: a review of ion-sample interaction. *Microsc. Res. Techn.* **35**, 320–333.

Kuba J., Mitchels J., Hovorka M. *et al.* (2020) Advanced cryo-tomography workflow developments – correlative microscopy, milling automation and cryo-lift-out. *J. Microsc.* This issue.

Lamers, E.., Walboomers, X.F., Domanski, M. *et al.* (2011) Cryo dualbeam focused ion beam-scanning electron microscopy to evaluate the interface between cells and nanopatterned scaffolds. *Tissue Eng. C* **17**, 1–7.

Limmer, D.T. & Chandler, D. (2014) Theory of amorphous ices. *PNAS* **111**, 9413–9418.

Mahamid, J., Schampers, R., Persoon, H., Hyman, A.A., Baumeister, W. & Plitzko, J.M. (2015) A focused ion beam milling and lift-out approach for site-specific preparation of frozen-hydrated lamellas from multicellular organisms. *J. Struct. Biol.* **192**, 262–269.

Marko, M., Hsieh, C., Moberlychan, W., Mannella, C.A. & Frank, J. (2005) Focused ion beam milling of vitreous water: prospects for an alternative to cryo-ultramicrotomy of frozenhydrated biological samples. *J. Microsc.* **222**, 42–47.

Martelli, F., Torquato, S., Giovambattista, N. & Car, R. (2017) Large-scale structure and hyperuniformity of amorphous ices. *PRL* **119**, 136002.

McDonald, K. (2007) Cryo-preparation methods for electron microscopy of selected model systems. *Meth. Cell Biol.* **79**, 23–56.

Medeiros, J.M., Böck, D. & Pilhofer, M. (2018) Imaging bacteria inside their host by cryo-focused ion beam milling and electron cryo-tomography. *Curr. Opin. Microbiol.* **42**, 62–68.

Medeiros, J.M., Böck, D., Weiss, G.L., Kooger, R., Wepf, R.A. & Pilhofer, M. (2018a) Robust workflow and instrumentation for cryo-focused ion beam milling of samples for electron cryo-tomography. *Ultramicroscopy* **190**, 1–11.

Meister, K., Strazdaite, S., DeVries, A.L., Lotze, S., Olijve, L.L.C., Voets, I.K. & Bakker, H.J. (2014) Observation of ice-like water layers at an aqueous protein surface. *PNAS* **111**, 17732–17736.

Mielanczyk, L., Matysiak, N., Michalski, M., Buldak, R. & Wojnicz, R. (2014) Closer to the native state. Critical evaluation of cryo-techniques for transmission electron microscopy: preparation of biological samples. *Fol. Histoch. Cytochem.* **52**, 1–17.

Möbius, W., Cooper, B., Kaufmann, W.A., Imig, C., Ruhwedel, T., Snaidero, N., Saab, A.S. & Varoqueaux, F. (2010) Electron microscopy of the mouse central nervous system. *Meth. Cell Biol.* **96**, 475–512.

Moor, H. (1987) *Theory and Practice of High Pressure Freezing*. Springer-Verlag, Berlin.

Mulders, J.J.L., De Winter, D.A.M. & Duinkerken, W.J.H.C.P. (2007) Measurements and calculations of FIB-milling yield of bulk metals. *Microelec. Eng.* **84**, 1540–1543.

Parmenter C. (2020) Cryo-FIB-lift-out: practically impossible to practical reality. *J. Micros.* This issue.

Reimer, L. (1998) *Scanning Electron Microscopy, Physics of image formation and microanalysis*, 2nd edn. Springer, Heidelberg, ISBN 978-3-540-38967-5.

Rigort, A., Bäuerlein, F.J.B., Laugks, T. *et al*. (2010a) A 360° rotatable Cryo-FIB stage for micromachining frozen-hydrated specimens for cryo-electron tomography. *Microsc. Microanal.* **16**(Suppl 2), http://doi.org/10.1017/S1431927610058186.

Rigort, A., Bäuerlein, F.J.B., Leis, A. *et al*. (2010b) Micromachining tools and correlative approaches for cellular cryo-electron tomography. *J. Struct. Biol.* **172**, 169–179.

Rigort, A., Bäuerlein, F.J.B., Villa, E., Eibauer, M., Laugks, T., Baumeister, W. & Plitzko, J.M. (2012) Focused ion beam micromachining of eukaryotic cells for cryo-electron tomography. *PNAS* **109**, 4449–4454.

Rubino, S., Akhtar, S., Melin, P., Searle, A., Spellward, P. & Leifer, K. (2012) A site-specific focused-ion-beam lift-out method for cryo-transmission electron Microscopy. *J. Struct. Biol.* **180**, 572–576.

Ryan, K.P., Purse, D.H., Robinson, S.G. & Wood, J.W. (1987), The relative efficiency of cryogens used for plunge-cooling biological specimens. *J. Microsc.* **145**, 89–96.

Sartori-Rupp, A., Cervantes, D.C., Pepe, A. *et al*. (2019) Correlative cryo-electron microscopy reveals the structure of TNTs in neuronal cells. *Nat. Comm.* **10**, 342.

Schaffer, M., Mahamid, J., Engel, B.D., Laugks, T., Baumeister, W. & Plitzko, J.M. (2017) Optimized cryo-focused ion beam sample preparation aimed at in situ structural studies of membrane proteins. *J. Struct. Biol.* **197**, 73–82.

Schaffer, M., Pfeffer, S., Mahamid, J. *et al*. (2019) A cryo-FIB lift-out technique enables molecular-resolution cryo-ET within native *Caenorhabditis elegans* tissue. *Nat Methods* **16**, 757–762.

Schaffer, M., Schaffer, B. & Ramasse, Q. (2012) Sample preparation for atomic-resolution STEM at low voltages by FIB. *Ultramicroscopy* **114**, 62–71.

Schatten, H. (2012) The role of scanning electron microscopy in cell and molecular biology. *Scanning Electron Microscopy for the Life Sciences* (ed. by H. Schatten), pp. 1–15. Cambridge University Press, ISBN: 9780521195997.

Schertel, A., Snaidero, N., Han, H-M., Ruhwedel, T., Laue, M., Grabenbauer, M. & Möbius, W. (2013) Cryo-FIB-SEM: Volume imaging of cellular ultrastructure in native frozen specimens. *J. Struct. Biol.* **184**, 355–360.

Shorubalko, I., Choi, K., Stiefel, M. & Park, H.G. (2017) Ion beam profiling from the interaction with a freestanding 2D layer. *Beilstein J. Nanotechnol.* **8**, 682–687.

Spehner, D., Steyer, A.M., Bertinetti, L., Orlov, I., Benoit, L., Pernet-Gallay, K., Schertel, A. & Schultz, P. (2020) Cryo-FIB-SEM as a promising tool for localizing proteins in 3D. *J. Struct. Biol.* **211**, 107528.

Steyer, A.M., Schertel, A., Nardis, C. & Möbius, W. (2019) FIB-SEM of mouse nervous tissue: Fast and slow sample preparation. *Meth. Cell Biol.* **152**, 1–21.

Strunk, K.M., Wang, K., Ke, D., Gray, J.L. & Zhang, P. (2012) Thinning of large mammalian cells for cryo-TEM characterization by cryo-FIB-milling. *J. Microsc.* **247**, 220–227.

Szent-Györgyi, A. (1979) Welcoming address. *Cell-Associated Water* (ed. by W. Drost-Hansen & J.S. Clegg), pp. 1–2. Academic Press, New York.

Tivol, W.F., Briegel, A. & Jensen, G.J. (2008) An improved cryogen for plunge freezing. *Microc. Microanal.* **14**, 375–379.

Tros, M., Zheng, L., Hunger, J., Bonn, M., Bonn, D., Smits, G.J. & Woutersen, S. (2017) Picosecond orientation dynamics of water in living cells. *Nat. Commun.* **8**, 904.

Umrath, W. (1974) Cooling bath for rapid freezing in electron microscopy. *J. Microsc.* **101**, 103–105.

Vidavsky, N., Akiva, A., Kaplan-Ashiri, I., Rechav, K., Addadi, L., Weiner, S. & Schertel, A. (2016) Cryo-FIB-SEM serial milling and block face imaging: large volume structural analysis of biological tissues preserved close to their native state. *J. Struct. Biol.* **196**, 487–495.

Volkert, C.A. & Minor, A.M. (2007) Focused ion beam microscopy and micromachining. *MRS Bulletin* **32**, 389–395.

Walther, P. (2003) Recent progress in freeze-fracturing of high-pressure frozen samples. *J. Microsc.* **212**, 34–43.

Wang, K., Strunk, K., Zhao, G., Gray, J.L. & Zhang, P. (2012) 3D structure determination of native mammalian cells using cryo-FIB and cryo-electron tomography. *J Struct. Biol.* **180**, 318–326.

Weikusat, I., De Winter, D.A.M., Pennock, G.M., Hayles, M.F., Schneijdenberg, C.T.W.M. & Drury, M.R. (2011) Cryogenic EBSD on ice: preserving a stable surface in a low pressure SEM. *J. Microsc.* **242**, 295–310.

Weiss, G.L., Kieninger, A.-K., Maldener, I., Forchhammer, K. & Pilhofer, M. (2019) Structure and function of a bacterial gap junction analog. *Cell* **178**, 374–384.

Wolff, A., Klingner, N., Thompson, W., Zhou, Y., Lin, J., Peng, Y.Y., Ramshaw, J.A.M. & Xiao, Y. (2018) Modelling of focused ion beam induced increases in sample temperature: a case study of heat damage in biological samples. *J. Microsc.* **272**, 47–59.

Wolff, G., Limpens, R.W.A.L., Zheng, S., Snijder, E.J., Agard, D.A., Koster, A.J. & Bárcena, M. (2019) Mind the gap: Micro-expansion joints drastically decrease the bending of FIB-milled cryo-lamellae. *J. Struct. Biol.* **208**, 107389.

Zanil, M.S., Yi, H. & Puri, V. (2015) The mechanical properties of plant cell walls soft material at the subcellular scale: the implications of water and of the intercellular boundaries. *J. Mater. Sci.* **50**, 6608–6623.

Zhang, J., Ji, G., Huang, X., Xu, W. & Sun, F. (2016) An improved cryo-FIB method for fabrication of frozen hydrated lamella. *J. Struct. Biol.* **194**, 218–223.

Zuber, B., Nikonenko, I., Klauser, P., Muller, D. & Dubochet, J. (2005) The mammalian central nervous synaptic cleft contains a high density of periodically organized complexes. *PNAS* **102**, 19192–19197.